Natural Hazards in the Boundary Bay Region of the Strait of Georgia: A Compilation and Summary of Observations and Numerical Modeling Studies

Alexander Rabinovich, Richard Thomson and Nicky Hastings

Fisheries and Oceans Canada
Institute of Ocean Sciences
9860 West Saanich Road
Sidney, BC V8L 4B2

2023

Canadian Technical Report of Hydrography and Ocean Sciences 366

Fisheries and Oceans Canada Pêches et Océans Canada

Canada

Canadian Technical Report of Hydrography and Ocean Sciences

Technical reports contain scientific and technical information of a type that represents a contribution to existing knowledge, but which is not normally found in the primary literature. The subject matter is generally related to programs and interests of the Oceans and Science sectors of Fisheries and Oceans Canada.

Technical reports may be cited as full publications. The correct citation appears above the abstract of each report. Each report is abstracted in the data base Aquatic Sciences and Fisheries Abstracts.

Technical reports are produced regionally but are numbered nationally. Requests for individual reports will be filled by the issuing establishment listed on the front cover and title page.

Regional and headquarters establishments of Ocean Science and Surveys ceased publication of their various report series as of December 1981. A complete listing of these publications and the last number issued under each title are published in the Canadian Journal of Fisheries and Aquatic Sciences, Volume 38: Index to Publications 1981. The current series began with Report Number 1 in January 1982.

Rapport technique canadien sur l'hydrographie et les sciences océaniques

Les rapports techniques contiennent des renseignements scientifiques et techniques qui constituent une contribution aux connaissances actuelles mais que l'on ne trouve pas normalement dans les revues scientifiques. Le sujet est généralement rattaché aux programmes et intérêts des secteurs des Océans et des Sciences de Pêches et Océans Canada.

Les rapports techniques peuvent être cités comme des publications à part entière. Le titre exact figure au-dessus du résumé de chaque rapport. Les rapports techniques sont résumés dans la base de données Résumés des sciences aquatiques et halieutiques.

Les rapports techniques sont produits à l'échelon régional, mais numérotés à l'échelon national. Les demandes de rapports seront satisfaites par l'établissement auteur dont le nom figure sur la couverture et la page de titre.

Les établissements de l’ancien secteur des Sciences et Levés océaniques dans les régions et à l'administration centrale ont cessé de publier leurs diverses séries de rapports en décembre 1981. Vous trouverez dans l'index des publications du volume 38 du Journal canadien des sciences halieutiques et aquatiques, la liste de ces publications ainsi que le dernier numéro paru dans chaque catégorie. La nouvelle série a commencé avec la publication du rapport numéro 1 en janvier 1982.

Canadian Technical Report of
Hydrography and Ocean Sciences 366

2023

NATURAL HAZARDS IN THE BOUNDARY BAY REGION OF THE STRAIT OF GEORGIA: A COMPILATION AND SUMMARY OF OBSERVATIONS AND NUMERICAL MODELING STUDIES

Alexander Rabinovich[1], Richard Thomson[1] and Nicky Hastings[2]

[1]Fisheries and Oceans Canada
Institute of Ocean Sciences
9860 West Saanich Road
Sidney, BC V8L 4B2

[2]Natural Resources Canada
Geological Survey of Canada - Pacific Division
605 Robson Street
Vancouver, BC V6B 5J3

Cat. No. Fs97-18/366E-PDF ISBN 978-0-660-68512-0 ISSN 1488-5417

Correct citation for this publication:

Rabinovich, A., Thomson, R., and Hastings, N., 2023. Natural hazards in the Boundary Bay region of the Strait of Georgia: A compilation and summary of observations and numerical modeling studies. Can. Tech. Rep. Hydrogr. Ocean Sci. 366: v + 37 p.

CONTENTS

ABSTRACT

Rabinovich, A., Thomson, R., and Hastings, N., 2023. Natural hazards in the Boundary Bay region of the Strait of Georgia: A compilation and summary of observations and numerical modeling studies. Can. Tech. Rep. Hydrogr. Ocean Sci. 366: v + 37 p.

This study examines the risk to southwestern British Columbia from hazardous sea level events, with focus on the Boundary Bay region. We identify five main types of marine hazard affecting sea levels in the study region: (1) Trans-oceanic tsunamis; (2) local tsunamis; (3) landslide-generated tsunamis; (4) storm surges; and (5) meteorological tsunamis.

Trans-oceanic tsunamis generated at the Cascadia and Alaska-Aleutian subduction zones pose the highest risk to the region. A Cascadia Subduction Zone failure could generate wave amplitudes of up to 1.5 m in northwestern Boundary Bay and 1.3 m along the Semiahmoo coast. Associated currents could reach 3 m/s at the Drayton Harbor entrance and 2 m/s at the mouth of Campbell River. The risk from a major Alaska-earthquake tsunami is considerably lower. Because of sheltering by the Gulf and San Juan islands, tsunamis triggered by sources in the Strait of Georgia and Puget Sound are considered lesser risks to the Boundary Bay region.

Storm surges could reach 0.6 m above tide levels in northwestern Boundary Bay and around 0.5 m at Semiahmoo First Nations sites. Meteorological tsunamis (tsunami-like waves generated by atmospheric processes) pose a minor risk to the study region. In contrast, a sudden failure of the large body of unconsolidated alluvial sediments in the vicinity of Roberts Bank (Fraser River Delta) or deposits on the north slope of Orcas Island (San Juan Islands) could trigger hazardous landslide-generated tsunamis in the southern Strait of Georgia.

RÉSUMÉ

Rabinovich, A., Thomson, R., and Hastings, N., 2023. Natural hazards in the Boundary Bay region of the Strait of Georgia: A compilation and summary of observations and numerical modeling studies. Can. Tech. Rep. Hydrogr. Ocean Sci. 366: v + 37 p.

Cette étude examine le risque que représentent pour le sud-ouest de la Colombie-Britannique les événements dangereux liés au niveau de la mer, en mettant l'accent sur la région de Boundary Bay. Nous identifions cinq principaux types de risques marins affectant le niveau de la mer dans la région d'étude: (1) les tsunamis transocéaniques; (2) les tsunamis locaux; (3) les tsunamis générés par des glissements de terrain; (4) les ondes de tempête; et (5) les tsunamis météorologiques.

Les tsunamis transocéaniques générés dans les zones de subduction Cascadia et Alaska-Aléoutiennes présentent le risque le plus élevé pour la région. Une défaillance de la zone de subduction de Cascadia pourrait générer des amplitudes de vagues allant jusqu'à 1,5 m dans le nord-ouest de Boundary Bay et 1,3 m le long de la côte de Semiahmoo. Les courants associés pourraient atteindre 3 m/s à l'entrée du port de Drayton et 2 m/s à l'embouchure de Campbell River. Le risque d'un tsunami sismique majeur en Alaska est considérablement plus faible. En raison de l'abri offert par les îles du Golfe et de San Juan, les tsunamis déclenchés par des sources situées dans le détroit de Georgia et Puget Sound sont considérés comme présentant des risques moindres pour la région de Boundary Bay.

Les ondes de tempête pourraient atteindre 0,6 m au-dessus du niveau de la marée dans le nord-ouest de Boundary Bay et environ 0,5 m sur les sites des Premières Nations de Semiahmoo. Les tsunamis météorologiques (vagues de type tsunami générées par des processus atmosphériques) présentent un risque mineur pour la région étudiée. En revanche, une rupture soudaine d'une grande masse de sédiments alluviaux non consolidés à proximité de Roberts Bank (delta du fleuve Fraser) ou de dépôts sur le versant nord de l'île Orcas (îles San Juan) pourrait déclencher de dangereux tsunamis générés par des glissements de terrain dans le sud du détroit de Géorgie.

1. INTRODUCTION

Large segments of the British Columbia coast are susceptible to tsunamis generated by major earthquakes within the Pacific Ocean and by local underwater earthquakes. The catastrophic tsunamis of the last two decades demonstrate the serious threat of major seismically generated tsunamis to coastal communities in southern British Columbia [cf. *Clague et al.* 2003; *Leonard et al.*, 2014]. The Strait of Georgia, including Boundary Bay, is partially sheltered from tsunami waves incoming from the open ocean; nevertheless, tsunamis from major events (e.g., the 1964 Alaska and 2011 Tohoku tsunamis) have penetrated into the region and have been recorded there by CHS and NOAA tide gauges. Moreover, Vancouver Island and the adjacent mainland coast are seismically active regions; the 1946 Vancouver Island Earthquake (M_w 7.3) generated local tsunamis in the Strait of Georgia that created considerable damage and killed one person. Additional risk for this region is associated with landslide generated tsunamis, meteorological tsunamis and storm surges. Several events associated with these phenomena have been observed in the past and can occur in the future. The long-term prediction and possible mitigation of marine floods associated with these phenomena are vitally important, especially for areas being considered for new construction or major renovations [*Leonard et al.*, 2014].

In general, there are the following types of marine hazardous sea level events that potentially can affect the area of Boundary Bay, British Columbia (BC):

(1) Major trans-oceanic tsunamis

(2) Local tsunamis

(3) Landslide-generated tsunamis

(4) Storm surges

(5) Meteorological tsunamis

These five types of phenomena for the southern Strait of Georgia, and specifically for the Boundary Bay region, have been examined in a number of IOS reports based both on analyses of available observational data and numerical modelling [*Rabinovich et al*., 2019a, 2020a, 2020c; *Fine and Thomson*, 2020a, 2020b, 2020c]. The current report presents a summary of major results and findings from these reports. We have further augmented the findings from these studies using reports of *González et al.* [2003], *Forseth* [2006], [*Rabinovich et al*., 2020b] and several recent papers, including *Soontiens et al*. [2016], *Zhai et al*. [2019], *Rabinovich et al*. [2019b, 2021] and *Nemati et al*. [2023].

2. OBSERVATIONS

The observational data used in the present report are mainly from the Canadian Hydrographic Service (CHS) tide gauge records from instruments located in the southern part of the Strait of Georgia and at the head of Juan de Fuca Strait (Figure 1). Before the end of the 1990s, all stations were analogue ("pen-and-paper") instruments. As a result of destructive tsunamis in the 1990s in the Pacific Ocean, the CHS in 1997 initiated a major upgrade of the existing network of tide gauges on the BC coast, including those located in the Strait of Georgia. The new digital instruments were designed to continuously measure sea levels with much higher precision and time resolution than earlier analogue gauges, and to store recorded values with 1-min sampling interval increment [*Rabinovich and Stephenson,* 2004].

The Point Atkinson station, located on the northern coast of Burrard Inlet, at the entrance to the Strait of Georgia (Figure 1a), is one of the oldest CHS stations. Observations at the site started in 1914, so that the sea level record at this station is one of the longest for the coast of British Columbia [*Rabinovich et al.,* 2019b]. This station is the nearest CHS tide gauge station to the Boundary Bay area and is used in the present study as the main *reference station*. For approximately 85 years, the records from the Point Atkinson tide gauge were analogue, but since 1998 they have been digital. This means that for this station, almost 22 years of continuous 1-min data have been collected, which can be used to examine processes in a broad frequency range, including local seiches and meteotsunamis.

Additionally, we have used data from several NOAA (USA) tide gauge (TG) stations located in the southern Strait of Georgia and Juan de Fuca Strait (Figure 1), in particular, Cherry Point and Friday Harbor. The Cherry Point tide gauge is located on the mainland of Washington State, approximately 25 km south of Boundary Bay; Friday Harbor is located on San Juan Island, about 35 km from Boundary Bay (Figures 1a,b). The Friday Harbor TG (NOAA #944-9880) was installed in 1932 and the Cherry Point TG (#944-9424) was installed in 1971. Until 1995, both instruments were analogue, but were replaced by digital TGs with a sampling interval of 6 min at the end of 1995. Since 1 January 2008, both instruments have been continuously working with 1-min sampling. Both stations were also used by *Rabinovich et al.* [2019a] as the reference for Boundary Bay.

In addition to coastal TGs, we have used data from two ONC Victoria Experimental Network Under the Sea (VENUS) sites. One of them (V1), is located in the southern part of the Strait of Georgia in close vicinity to Boundary Bay, while the other (V2) is located in Saanich Inlet near the Patricia Bay TG (Figure 1). Both stations have been in operation since February 2006; the data are available with a time step of 1 min.

The last set of data added to the present study is from the meteorological "school network", a unique set of high-resolution atmospheric records from 132 stations located in schools on southern Vancouver Island and nearby islands [*Weaver and Wiebe*, 2006]. Here, we mainly used stations located relatively close to Boundary Bay, i.e., in the Saanich Peninsula and the Gulf Islands [*Rabinovich et al.*, 2020b]. These instruments enable us to examine both the spatial and temporal structure of mesoscale atmospheric disturbances during specific meteotsunami events and also to estimate the general characteristics of atmospheric processes in this region.

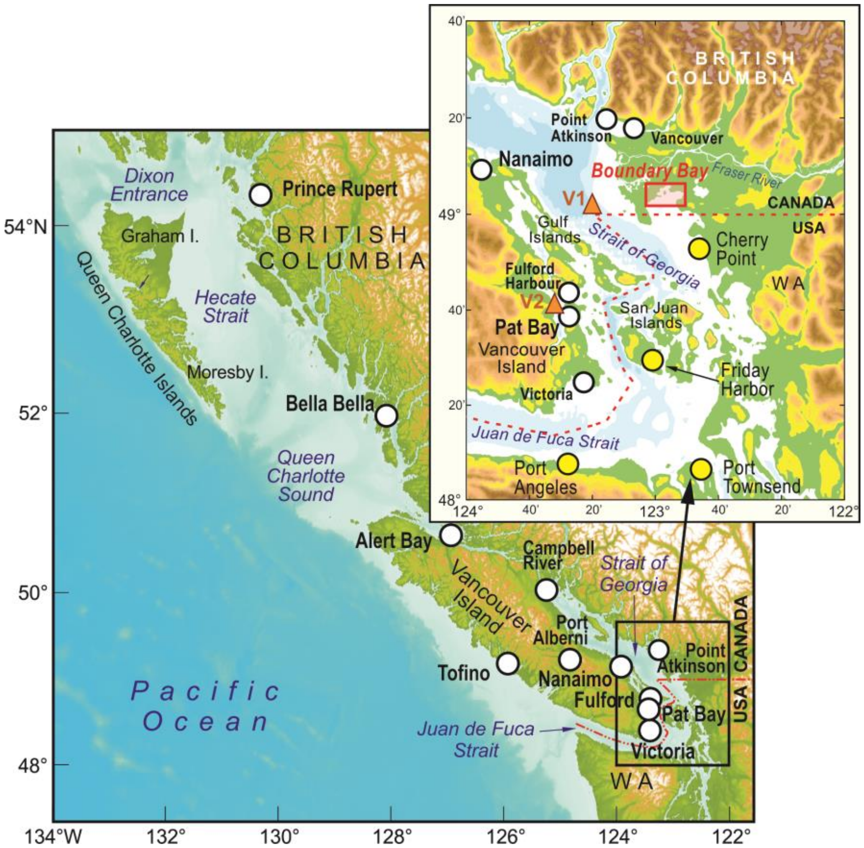

Figure 1. Map of British Columbia with locations of the Canadian Hydrographic Service (CHS) (*white circles*) and NOAA (*yellow circles*) coastal tide gauges; *orange triangles* denote ONC VENUS bottom pressure stations. The Boundary Bay area is indicated in the inset by the *red rectangular*.

3. HISTORICAL AND RECENT TRANS-OCEANIC TSUNAMIS

Trans-oceanic tsunamis are a major threat for coastal areas of the world ocean, including British Columbia. The Great Chilean tsunami of 22 May 1960 crossed the Pacific Ocean and killed 61 people on the Hawaiian Islands, 32 in the Philippines and 142 in Japan [cf. *Rabinovich et al.*, 2019b]. The 2004 Sumatra tsunami killed 230,00 people in 14 countries, including South Africa located 6000 km from the source area. The Sumatra tsunami waves also went around Australia and New Zealand and reached the coasts of British Columbia and Alaska [*Rabinovich et al.*, 2006]. The moderate 2006 Kuril Islands tsunami crossed the Pacific and caused $20 million damage at Crescent City in California [*Dengler et al.*, 2008].

Although the outer coast of British Columbia is at high risk to trans-oceanic tsunamis, the southern Strait of Georgia (SoG) is relatively sheltered from incoming tsunami waves. *Rabinovich et al.* [2020b] examined all available information on Pacific tsunamis that could affect the coasts of the Strait of Georgia, including existing tsunami catalogues and specific papers, and found that only major trans-oceanic tsunamis can penetrate into this region. During the entire instrumental period of 1900-2020, there have been seven such events: (1) the 1946 Aleutian Islands tsunami (initiated by an earthquake with a momentum magnitude M_w 8.6); (2) the 1952 Kamchatka tsunami (M_w 9.0); (3) the 1957 Andreanof Islands (M_w 8.6); (4) the 1960 Great Chile tsunami (M_w 9.5); (5) the 1964 Alaska tsunami (M_w 9.2); (6) the 2010 Chile (Maule) tsunami (M_w 8.8); and (7) the 2011 Tohoku (East Japan) tsunami (M_w 9.0). Also, paleotsunami field surveys on the coasts of British Columbia, Washington and Oregon [cf. *Wang et al*., 2003; *Clague et al*., 2003] and historical chronicles in Japan [cf. *Atwater et al.*, 2005] show that this region was affected by a major tsunami generated in 1700 by a great Cascadia Subduction Zone (CSZ) earthquake with an estimated magnitude of M_w 9.0. The epicenters of all these eight major earthquakes are shown in Figure 2.

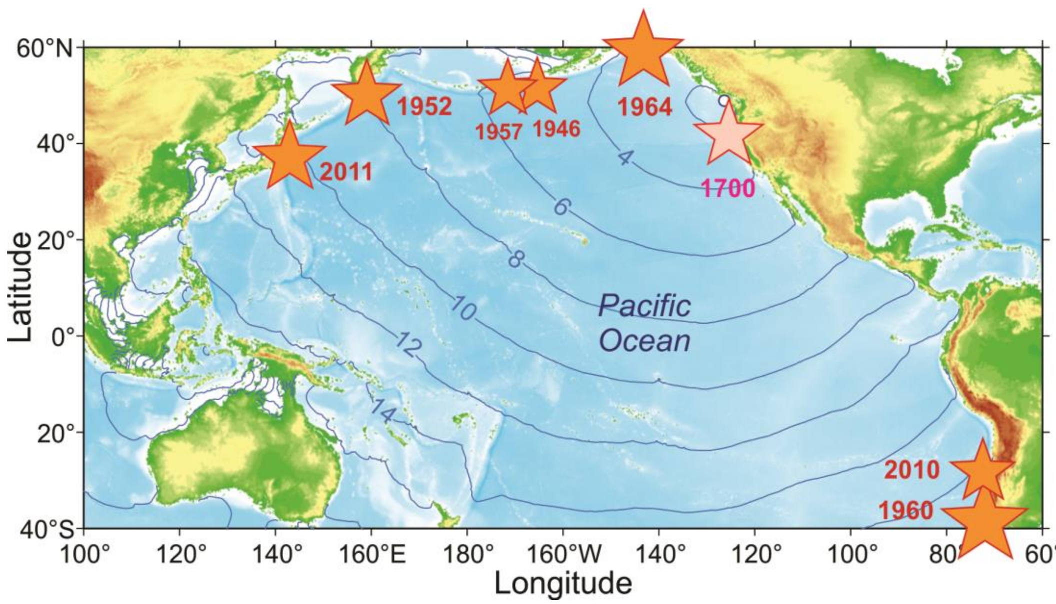

Figure 2. Epicenters (orange stars) of the five great earthquakes of the 20th century (1946 Aleutian Islands, 1952 Kamchatka, 1957 Andreanof Islands, 1960 Chile and 1964 Alaska) and the two of the 21st century (2010 Chile and 2011 Tohoku) in the Pacific Ocean that produced major trans-oceanic tsunamis. The size of the star is proportional to the earthquake magnitude (M_w). The solid blue lines are inverted isochrones of the tsunami travel time (in hours) from various parts in the Pacific Ocean to Tofino, British Columbia (denoted by the *white circle*). The epicenter of the 1700 Cascadia Subduction Zone earthquake is denoted by the pink star.

As indicated above, the San Juan and Gulf islands protect the SoG from arriving trans-oceanic waves. Therefore, the waves either do not penetrate into the region or they are strongly attenuated. Figure 3 shows maximum tsunami wave heights recorded during the last 110 years at Victoria and Point Atkinson. While the Victoria tide gauge recorded 39 tsunamis during this period, including all seven major events, the tide gauge at Point Atkinson recorded only three tsunamis (1960, 1964 and 2011), with measured tsunami trough-to-crest wave heights of 20, 28 and 5.8 cm, respectively; the corresponding amplitudes for these events relative to mean sea level were 12, 12 and 2.8 cm [*Rabinovich et al.*, 2019b], which were 5-10 times smaller than at the Victoria tide gauge.

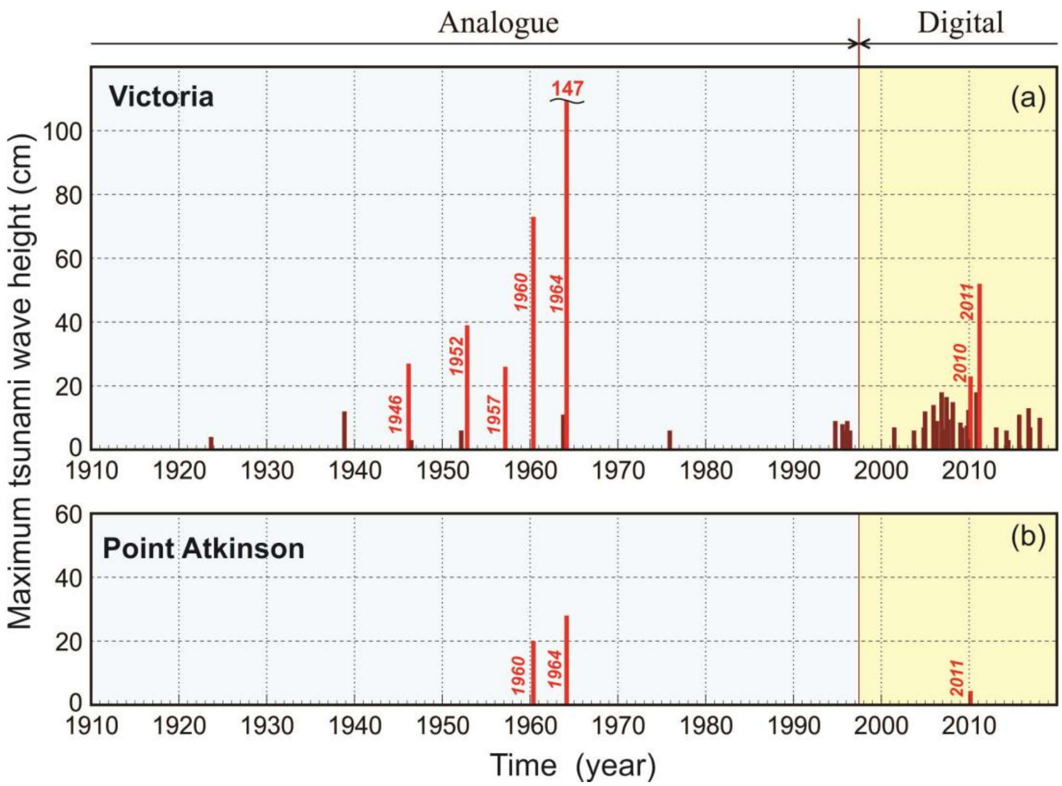

Figure 3. Maximum wave heights of tsunamis recorded at (a) Victoria and (b) Point Atkinson during the period 1910–2019. Up to 1997, measurements were made by analogue tide gauges; since July 1997, digital tide gauges have been used. Red bars indicate tsunami wave heights for the five great tsunamis of the 20th century (1946, 1952, 1957, 1960 and 1964) and two of the 21st century (2010 and 2011); all the others are indicated by magenta bars.

There have been no direct tsunami measurements in Boundary Bay. However, based on the above findings and on preliminary numerical modeling results, *Fine and Thomson* [2020a,b] concluded that the major threat for the Boundary Bay area is associated with great tsunamis generated in two specific source regions that actually are the closest to the coast of British Columbia: (1) the Cascadia Subduction Zone (i.e., the source of a 1700-like event) and (2) Alaska (the source of a 1964-like event), while other tsunami-source regions may be ignored. The numerical studies provide estimates of the expected maximum tsunami wave amplitudes related to these two types of events.

3.1. Modeling the 1700 Cascadia tsunami

The Cascadia Subduction Zone (CSZ) is a convergent plate boundary that stretches from central Vancouver Island (Canada) to Northern California (USA). It is here that the Explorer, Juan de Fuca, and Gorda plates slide eastward below the continental North American Plate (Figure 4). The Great CSZ earthquake of 26 January 1700, which had an estimated magnitude M_w = 9.0, generated a major trans-oceanic tsunami that caused significant destruction in Japan on the opposite side of the Pacific Ocean [cf. *Atwater et al.*, 2005], and strongly affected the outer coast of British Columbia. There is no reliable information or data concerning historical heights on the coast of British Columbia associated with this tsunami, however, paleotsunami findings on the coast of Vancouver Island and the west coast of the USA [cf. *Wang et al.*, 2003; *Clague et al*., 2000, 2003; *Wang et al.*, 2013] show that tsunami waves of ~15 m likely struck these coasts at the time of the 1700 CSZ earthquake.

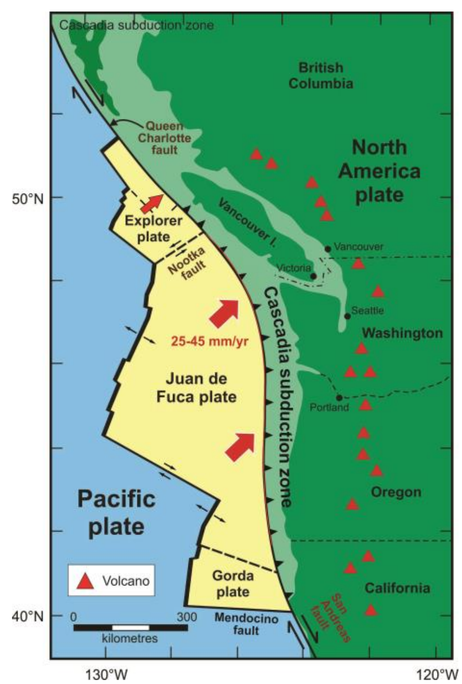

Figure 4. The Cascadia Subduction Zone (CSZ), a convergent plate boundary stretching 1000 km from northern Vancouver Island (BC) to northern California. The Juan de Fuca Plate and two smaller plates are sliding beneath the North American Plate.

A high-resolution, four-level, nested-grid tsunami model was used by *Fine and Thomson* [2020a] to simulate tsunami waves and wave-induced currents that will be generated in Boundary Bay in the southern Strait of Georgia by a CSZ earthquake with magnitude M_w = 9.0. Two versions of the earthquake-induced tsunami source region were used: Model A, a whole margin buried rupture; and Model B, a whole margin splay-faulting rupture (Figure 5). In the splay model (Model B), the rupture extends upward to the seafloor and hence has a greater effect on the overlying water [*Wang et al.*, 2013]. The spatial resolutions of the nested grids were ~1.8 km, 360 m, 60 m, and 10 m. The results of computations for Grid 3 (the Fraser River delta) and Grid 4 (Boundary Bay) for Models A and B are shown in Figure 6.

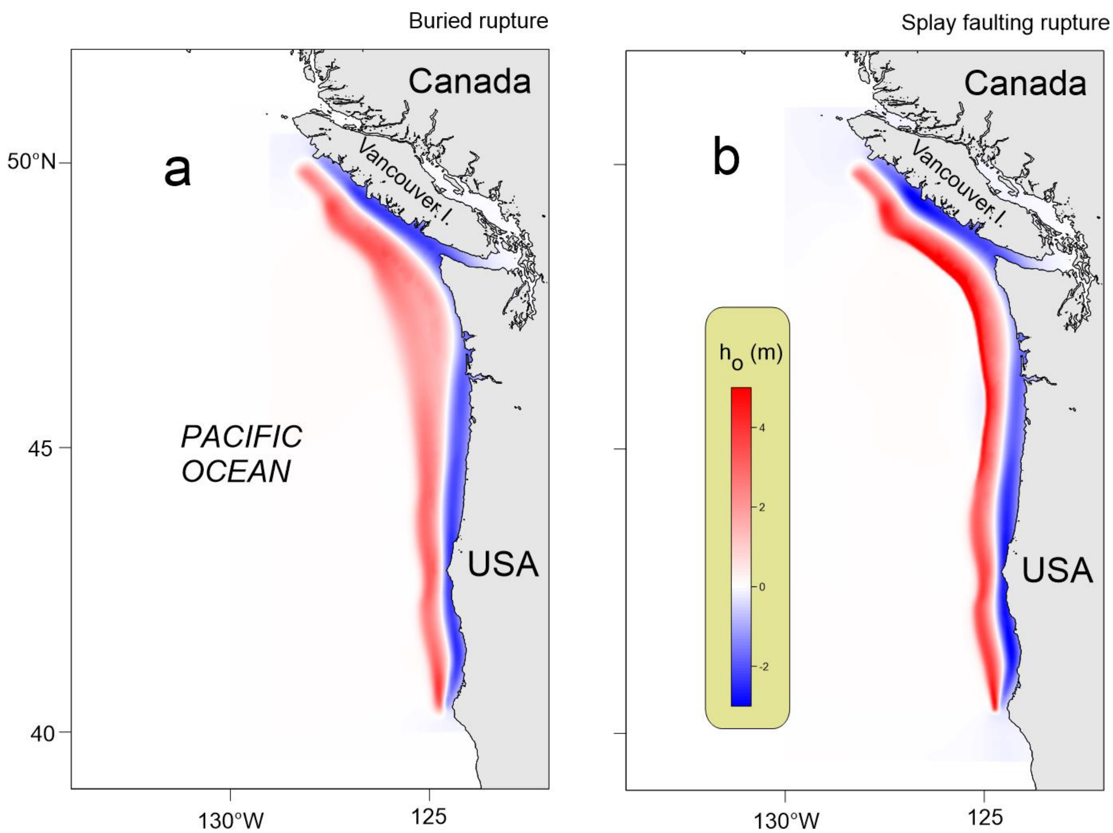

Figure 5. Maps of the Cascadia rupture zone tsunami sources according to *Gao* [2016]. Seafloor displacements, h_0, are in metres. (a) Whole margin buried rupture (Model A); and (b) Whole margin splay-faulting rupture (Model B). (From [*Fine and Thomson*, 2020a]).

Fine and Thomson [2020a] listed the following major results of their numerical modelling for the Boundary Bay area:

(1) Models A and B produce similar results in Boundary Bay, with Model A (the whole margin buried model) yielding slightly higher (by 2-7%) wave amplitudes than the whole margin splay-faulting rupture scenario (Model B). Boundary Bay is more exposed to tsunami waves from a CSZ earthquake than the coast of Metro Vancouver. For both models, the first wave to arrive is a wave trough, with sea level **dropping by 60-70 cm** within 2-2.5 hours after the start of the earthquake.

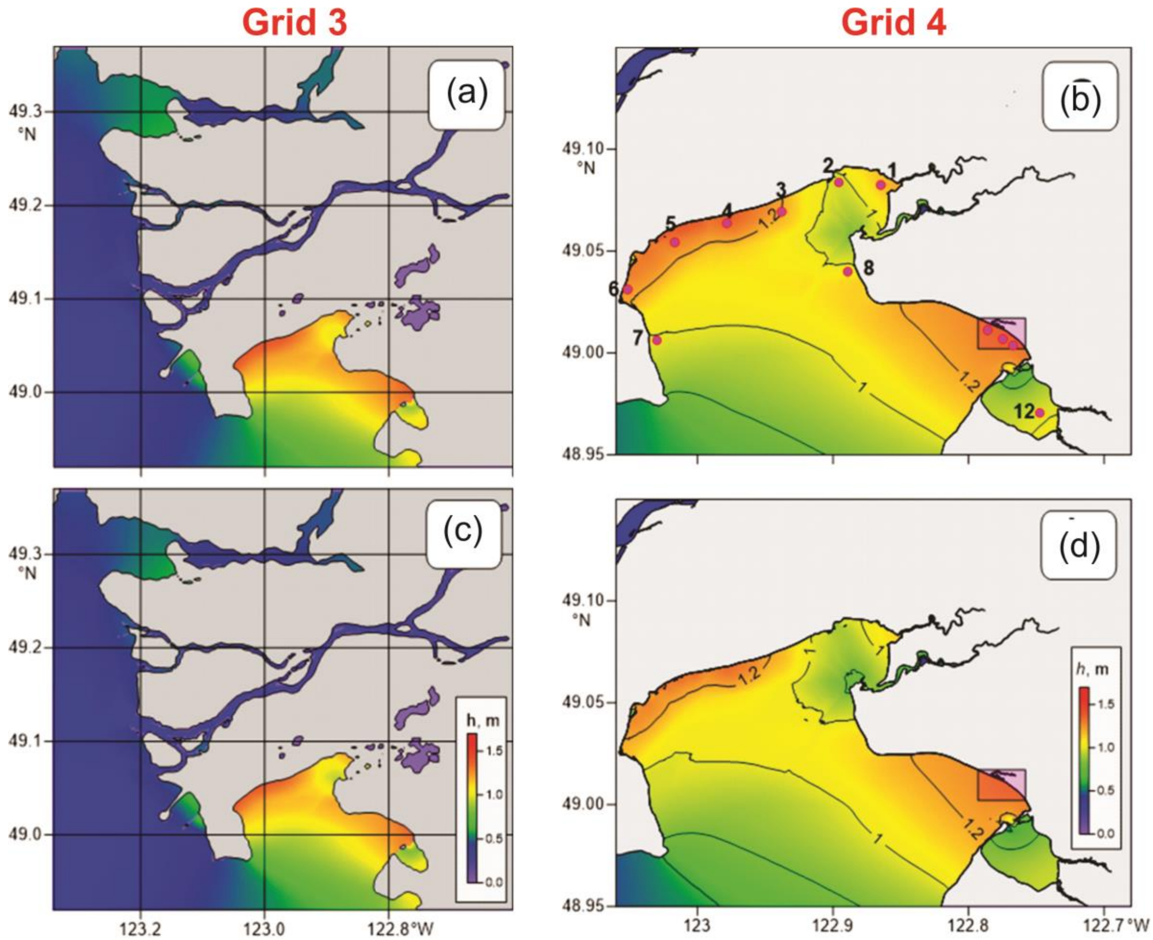

Figure 6. Spatial distribution of maximum computed tsunami wave heights (h, in metres) for (a) Model A, Grid 3; (b) Model A, Grid; (c) Model B, Grid 3 and (d) Model B, Grid 4. In (c) and (d), numbers in the Boundary Bay area denote sites for which tsunami wave records have been simulated (from [*Fine and Thomson*, 2020a]).

(2) The leading wave crest that immediately follows the initial drop in water level is the highest wave. It reaches a peak of **1.1-1.5 m** roughly 2:45 – 3:15 hours after the start of the earthquake. The major periods of tsunami waves in Boundary Bay and Semiahmoo Bay are 2-3 hours (dominant) and 1 hour (secondary, more pronounced in Model B).

(3) Wave heights are distributed nonuniformly within Boundary Bay. Maximum wave amplitudes (of **up to 1.5 m**) occur within the northwestern part on the Bay, and along the Semiahmoo coast (**up to 1.3 m**).

(4) The tsunami-induced ocean currents are typically **less than 1 m/s** in most areas but are **up to 3 m/s** at the entrance to Drayton Harbour and **up to 2 m/s** at the mouth of Campbell River on the Semiahmoo coast. Model B produced slightly stronger currents than Model A.

(5) Tsunami waves would cause flooding, mostly in the northwestern part of Boundary Bay. Flooding would be restricted by the presence of the elongated dike along the northern coast of the bay. Flooding in the Semiahmoo area will likely occur in the Campbell River valley but will have a limited effect.

In general, *Fine and Thomson* [2020a] indicate that, while the study region is not susceptible to major flooding from a CSZ tsunami, if they add a 50% safety factor (a typical engineering value [cf. *AECOM*, 2013]), there is a tsunami hazard to the Semiahmoo area but it will remain confined to the low-lying regions along the Campbell River.

3.2. The Alaska Tsunami of 28 March 1964

The magnitude (M_w) 9.2 Alaska earthquake of 28 March 1964 produced a catastrophic tsunami, the second strongest in the 20th century (after the magnitude 9.5 1960 Chilean tsunami). The maximum water rise was 20 m at the source and the event generated the strongest tsunami response ever observed on the coast of British Columbia [cf. *Rabinovich et al.*, 2019b]. The 1964 earthquake occurred within the Alaska-Aleutian megathrust zone, where the Pacific Plate subducts under the North American Plate (Figure 7). This zone has the greatest potential to generate destructive tsunamis and is one of the most seismically active fault zones in the North Pacific. The 1964 megathrust Alaska earthquake caused the most destructive tsunami in Alaskan history and, further south, strongly impacted the west coasts of the USA and Canada [cf. *Johnson et al.*, 1996; *Lander*, 1996]. The tsunami spread over the entire Pacific Ocean and was recorded by 18 instruments on the coast of British Columbia, including those in the Strait of Georgia, along the Fraser River and even in Pitt Lake [*Rabinovich et al.*, 2019b]. The tsunami caused about $10 million in damage (1964-dollar values), mainly at the twin towns of Alberni and Port Alberni, with the maximum tsunami run-up at Port Alberni of about 8 m [cf. *Rabinovich et al.*, 2019b].

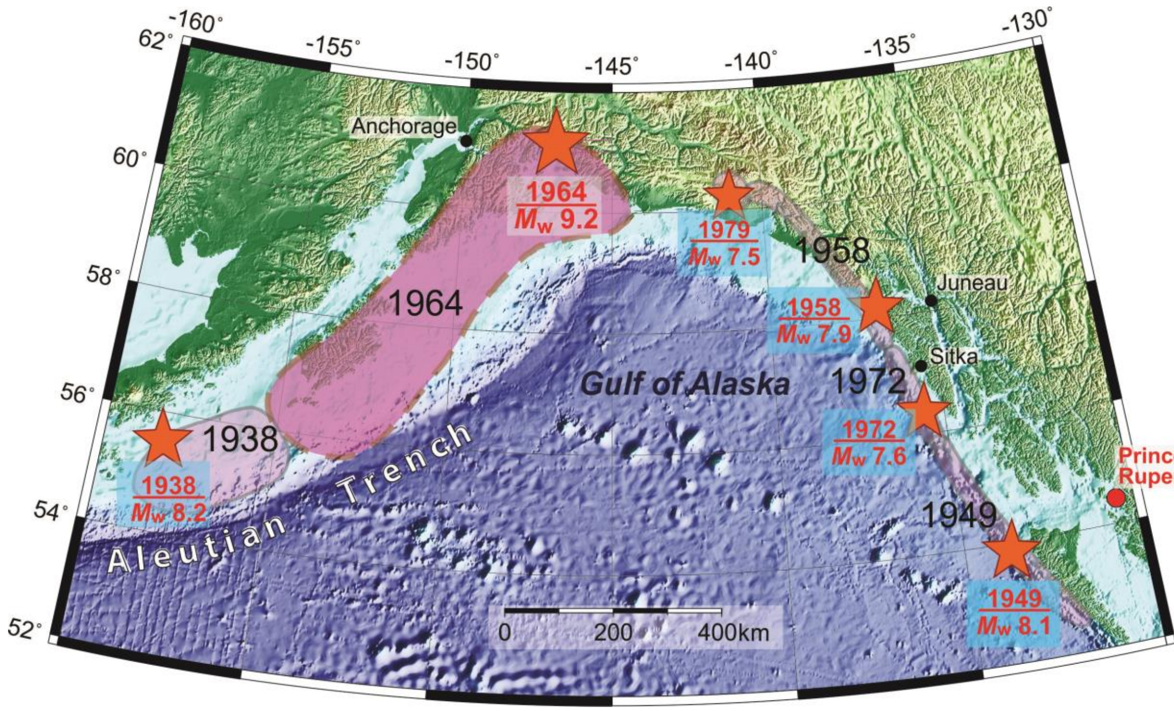

Figure 7. Map of south-central and southeastern Alaska with the rupture zones of six major historical earthquakes (shaded); the rupture zone of the 1964 Alaska earthquake is contoured by a thick brown dashed line. Red stars indicate epicenters of the earthquakes; the sizes of the stars are proportional to the earthquake magnitudes. Tide gauges at Sitka, Juneau and Anchorage are indicated by solid black circles; the red circle denotes the tide gauge at Prince Rupert. (From *Rabinovich et al.* [2019b]).

Several numerical models were constructed to simulate tsunami wave propagation from the 1964 source, including the coast of British Columbia [cf. *Dunbar et al.*, 1991; *Myers and Baptista*, 2001]. However, to estimate maximum possible tsunami wave heights and extreme tsunami-generated currents in the southern Strait of Georgia, more detailed high-resolution bathymetry, which became available recently, and a more refined source region were needed. The 1964 Alaska tsunami is typically considered as a proxy for a major future tsunami along the Pacific coast of North America

[*Suleimani et al*., 2013]. Therefore, to compute the expected tsunami waves for Boundary Bay, *Fine and Thomson* [2020b] applied an Alaska 1964-type earthquake M_w 9.2 source and used the same numerical model as for the 1700 CSZ event [*Fine and Thomson*, 2020a].

The high-resolution, nested-grid tsunami model used to simulate the distribution of tsunami waves and wave-induced currents that will be generated in Boundary Bay in the event of an 1964-type Alaska tsunami is based on an advanced tsunami source distribution [*Suleimani et al.*, 2013] and high-resolution bathymetry for the study area. The maximum computed tsunami wave heights are shown in Figure 8. The main results of the modelling study of *Fine and Thomson* [2020b] are the following:

(1) The tsunami at Boundary Bay will reach **0.45 m** above the tidal level at the time of the wave arrivals, with the first wave being the highest; tsunami waves of up to **0.35 m** are expected at the Semiahmoo coast.

(2) The distribution of tsunami wave amplitudes at the Boundary Bay will be nonuniform, with highest values at the end of the bay; in contrast, the distribution of waves amplitudes along the Semiahmoo coast will be nearly uniform.

(3) The tsunami will induce moderate currents at the entrance of Drayton Harbor (up to **1.5 m/s**) and at the mouth of Campbell River (up to **0.5 m/s**). At other locations, wave-indiced current will not exceed **0.3 m/s.**

Fine and Thomson [2020b] recommend the use of a safety factor of 50%, which should be added to the tsunami amplitudes estimated for a 1964-type event. However, even with such a factor, the risk of flooding in Boundary Bay by an Alaska 1964-type tsunami is low in comparison with a CSZ 1700-type tsunami.

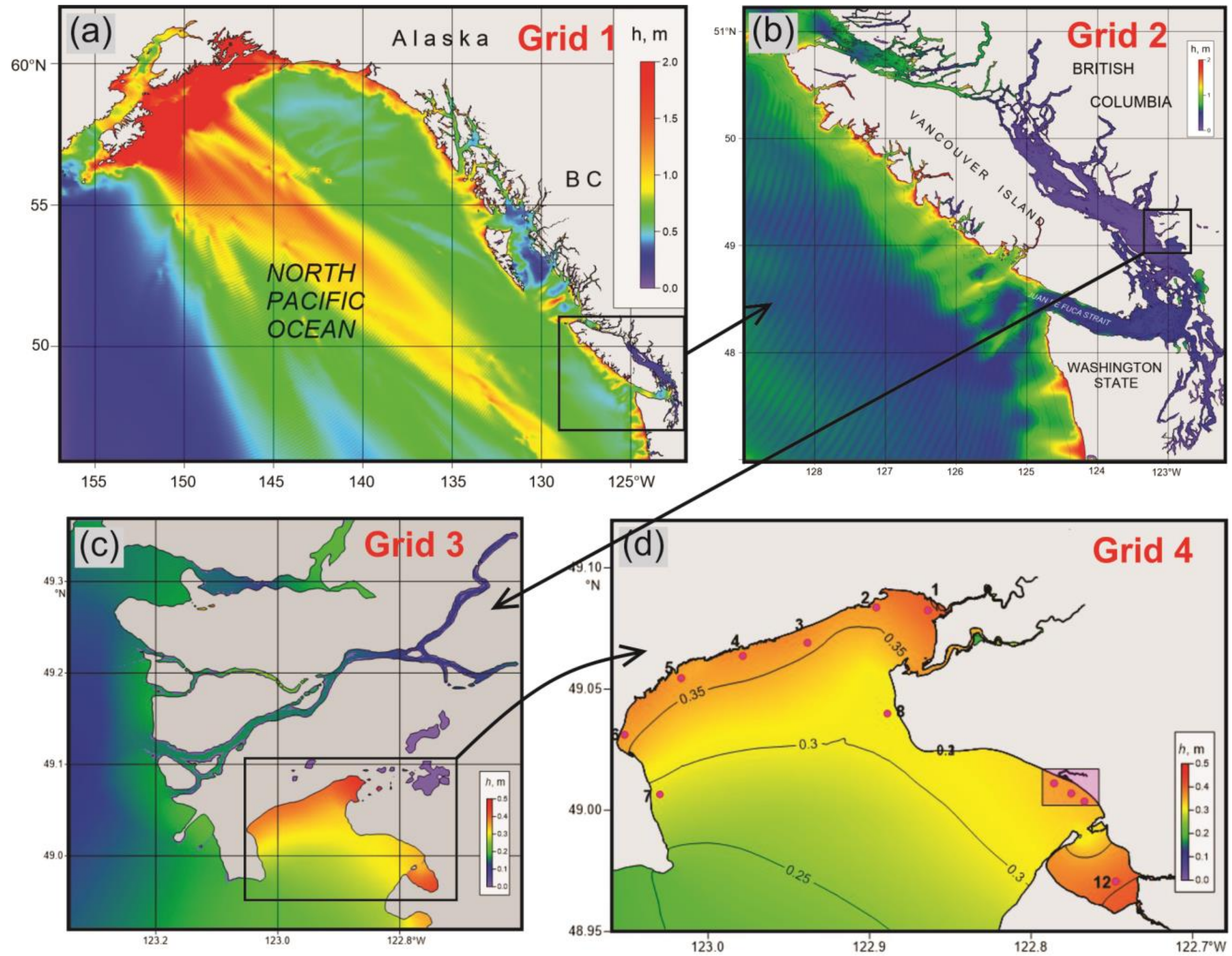

Figure 8. Distribution of maximum tsunami wave heights (metres) for (a) Grid 1, (b) Grid 2, (c) Grid 3 and (d) Grid 4 of the nested-grid model for waves generated by simulation of the 1964 tsunami. Numbers in (d) for Boundary Bay denote sites for which tsunami wave records have been simulated. (Modified from *Fine and Thomson* [2020b]).

4. LOCAL TSUNAMIS IN THE SOUTHERN STRAIT OF GEORGIA

The strongest tsunamigenic earthquakes in the Pacific region occur in major subduction zones bordering the Pacific Ocean that form the *Fire Rim*. All eight principal trans-oceanic tsunamis discussed in Section 3 were generated by great, M_w 8.6-9.5 earthquakes with source areas located in these zones. However, as noted earlier, the Strait of Georgia is strongly sheltered from incoming oceanic tsunamis by the San Juan and Gulf islands. That is why *Rabinovich et al.* [2020b] also considered the threat for this region from *local tsunamis*, i.e., from tsunamis generated by earthquakes with epicentres in the Strait of Georgia.

According to *Seemann et al.* [2011], the seismic zone of southern British Columbia includes three types of earthquakes: (1) shallow crustal earthquakes in the North America plate; (2) deeper sub-crustal earthquakes in the subducting Juan de Fuca plate; and (3) very large subduction interface earthquakes at the interface of the two plates. Most of the crustal earthquakes beneath Vancouver Island occur within approximately 20–30 km of the surface; most of them are small events. Significant earthquakes in the Strait of Georgia are very rare. The strongest damaging crustal earthquake in the region was the M_w 7.3 1946 event on eastern Vancouver Island (Figure 9) that a created a local tsunami [*Rogers*, 1980; *Stephenson et al.*, 2007].

This 1946 earthquake was Vancouver Island's largest historic earthquake (and Canada's largest historic onshore earthquake). The epicenter was located at 49.76°N, 125.34°W, about 16 km SSW from Campbell River. According to *Rogers and Hasegawa* [1978] and *Rogers* [1980], this earthquake did not produce a major tsunami. However, due to local landslides and slumping triggered by the earthquake, some minor water level disturbances occurred in coastal areas. The only casualty was associated specifically with one of these waves. At many places along the coast north of Campbell River the coastal waters were found to have increased in depth just offshore by up to 30 m.

Murty and Crean [1986] numerically simulated the 1946 Vancouver Island tsunami in the Strait of Georgia and adjacent parts of Johnstone and Juan de Fuca straits using the seismic motion diagram of *Rogers and Hasegawa* [1978] that showed a vertical ground uplift of up to 3 m. The indicated displacement was mostly on land, but part was in the Strait of Georgia. The grid size of the numerical model in both directions was 2.62 km, which was too coarse to resolve local topographic features and estimate possible resonant effects of the numerous bays, inlets and narrow channels, typical for this region. but it showed the general character of the tsunami. According to these simulations, there was no major Strait of Georgia-wide tsunami, but the water level disturbances were large enough to be noticeable. The computed tsunami wave heights at various locations along the west and east shores of the Strait of Georgia, including some islands, were from 0.4 to 2.7 m. For example, at Nanaimo the tsunami range was from -0.9 to +0.9 m, at Campbell River from -0.9 to +0.9 m, at Parksville from -0.2 to +0.3 m and at Vancouver (Burrard Inlet) from -0.8 to +0.7 m.

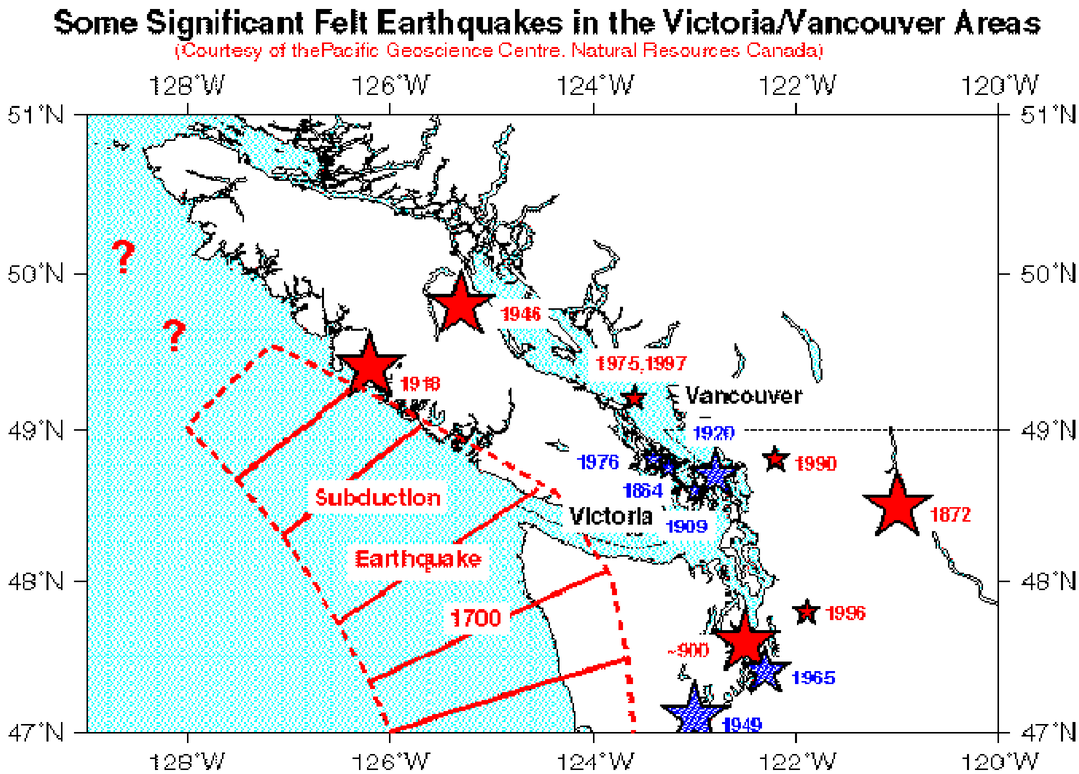

Figure 9. Map of significant earthquakes in the Victoria/Vancouver areas. *Red stars* denote indicate epicenters of earthquakes in the crust of the North America Plate; *blue stars* indicate earthquakes within the subducting Juan de Fuca Plate. The "belt" of epicenters located in bottom right part of the figure (900, 1949, 1965, 1996, etc.) are related to the Seattle Fault (Modified from *Rogers* [1998])

Murty and Hebenstreit [1989] developed a numerical model for the system consisting of the Strait of Georgia, Juan de Fuca Strait, and Puget Sound (GFP model). It is generally believed that the probability of major tsunamigenic earthquakes inside the GFP system is small. Nevertheless, *Murty and Hebenstreit* [1989] considered hypothetical earthquakes to occur off Victoria (in Juan de Fuca Strait), off Vancouver (in the Strait of Georgia), and off Seattle (in Puget Sound). The bottom motion used in these simulations approximated the corresponding sources for the 1946 event model taken from *Rogers and Hasegawa* [1978]. As expected, earthquakes occurring off the three cites produced greatest tsunami heights within their immediate source areas. Little wave energy in the model passes through to locations in the Strait of Georgia from the Victoria area earthquake simulation, although some effects were seen farther along Juan de Fuca Strait and in Puget Sound. The Vancouver area earthquake simulation produced the most moderate effects of the three simulations. However, the Gulf and San Juan islands effectively block tsunami entry into the Boundary Bay area from Juan de Fuca Strait and Puget Sound. The simulated earthquake off Seattle was shown to have little impact anywhere but in Puget Sound.

The major earthquakes known to have occurred in the Victoria/Vancouver areas are shown in Figure 9. Most of the prominent earthquakes in this region were focused along the Seattle Fault that crosses Puget Sound. For this reason, PMEL/NOAA and University of Washington tsunami scientists considered earthquake sources related to this fault when estimating the tsunami risk for Seattle and other cities located on the coast of Puget Sound [*González et al.*, 2003; *Walsh et al.*, 2003; 2014]. However, the San Juan and Gulf islands shelter the Strait of Georgia from tsunamis generated in this region.

5. LANDSLIDE-GENERATED TSUNAMIS IN THE STRAIT OF GEORGIA

Submarine landslides, slumps, rock-falls, and avalanches can generate significant tsunami waves in coastal areas of the World Ocean. Although landslide-generated tsunamis are much more localized than seismically generated tsunamis, they can produce destructive coastal run-up and cause severe damage, especially where the wave energy is trapped by the confines of inlets or semi-enclosed embayments.

The catastrophic event of 3 November 1994 in Skagway Harbor, Southeast Alaska initiated active investigations of landslide-generated tsunamis. The event began with the collapse of the PARN Dock that was under construction and led to a series of large amplitude waves estimated by eyewitnesses to have heights of 5-6 m in the harbour and 9-11 m at the shoreline [*Kulikov et al*., 1996]. The landslide and associated tsunami claimed the life of one PARN-Dock worker and caused an estimated $21 million damage [*Thomson et al*., 2001]. The event was the trigger for an intensive scientific discussion that eventually led to a greater understanding of slide/wave interaction and to substantial improvement in the numerical modelling of landslide-generated tsunamis. One of the lessons from the Skagway event was the necessity for a thorough examination and modelling of possible submarine sliding/slumping and slide-generated tsunamis in areas of new construction, especially those located in regions of moderate to large tidal ranges and in the vicinity of unstable sediment accumulations [*Bornhold and Thomson*, 2012].

In general, studies in the coastal areas of North America indicate high instability of certain coastal slopes and deltaic nearshore sediments [cf. *Johns et al*., 1986]. Large accumulations of unstable sediments deposited in the deltas of Alaska, British Columbia and Washington rivers, such as the Fraser, Skeena, and Nisqually, are particularly hazardous. Construction sites, buildings, and submarine cables in these areas are at considerable risk to direct damage from subaerial and submarine landslides. In these areas, tsunamis generated by the failure events probably pose an even greater threat in terms of damage and loss of life than tsunamis generated by earthquakes.

A specific area having high potential risk of possible underwater slope failure is Roberts Bank on the southern Fraser River delta, in the southern Strait of Georgia (Figure 10). Three factors have sparked interest in this area:

(1) The large volumes of unconsolidated sediments accumulated in the region;

(2) The possible risk of instability under earthquake loading;

(3) The presence of significant coastal infrastructure, including ferry terminals, port facilities, and electrical transmission cables.

This area is located quite close to Boundary Bay (Figure 10) and, potentially, a landslide tsunami generated in this region may affect the Boundary Bay area.

The Strait of Georgia is a long (222 km) and narrow (28 km) channel, with an average depth of about 155 m, separating Vancouver Island from the mainland of British Columbia. Freshwater discharge into the strait comes mainly from the Fraser River; the mouth of the Fraser River adjoins the Strait of Georgia along a 37-km delta front from Point Grey to Point Roberts Peninsula (Figure 10). The delta has been adding sediments at a high rate and forms deposits 100-200 m thick over glacial deposits. Roberts Bank, the main area of accumulated alluvial deposits, is located at the entrance of the South Arm of the delta between Sand Heads in the north and Point Roberts Peninsula in the south [*Thomson*, 1981]. The large unstable sediment mass (10^9 m^3) identified on the Roberts Bank slope [*Christian et al.*, 1997] could potentially result in significant submarine landslides and associated tsunamis and would likely produce severe damage.

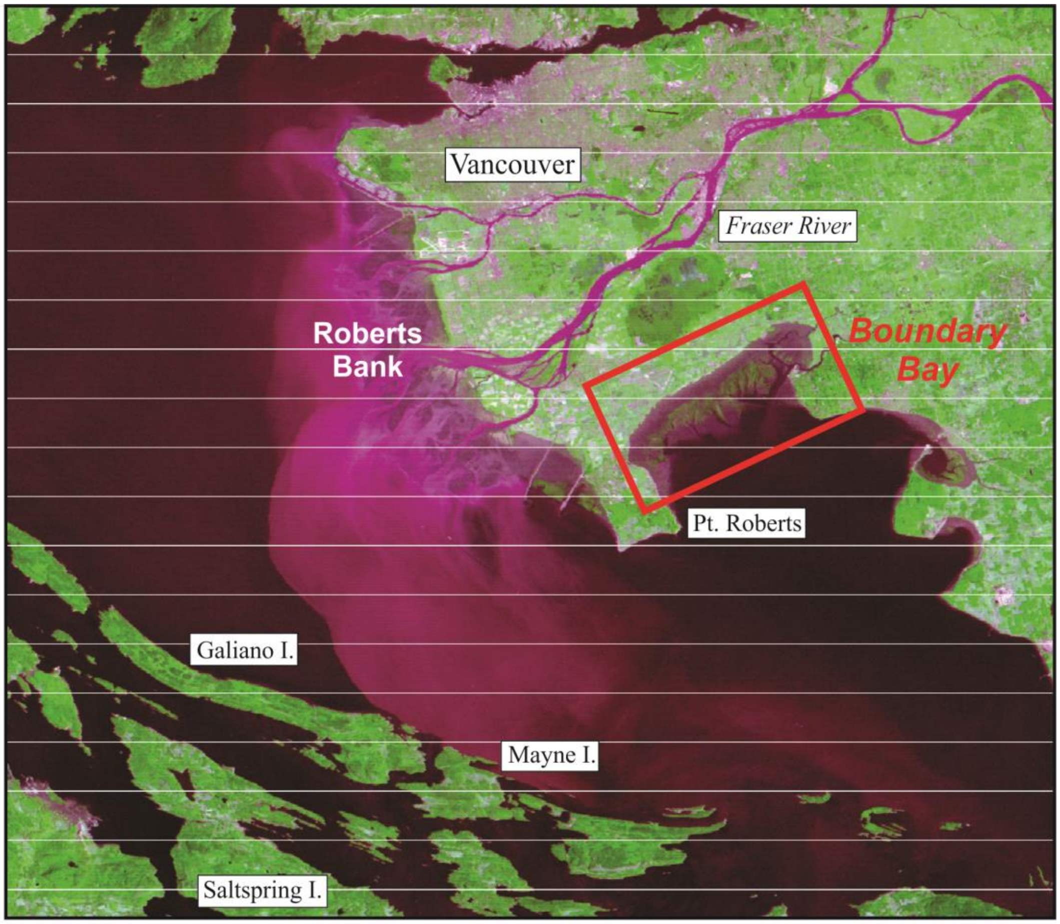

Figure 10. ERTS-1 satellite image of the Fraser River delta and plume on August 12, 1973. Spatial resolution is about 80 m. The colours are from infrared composite images showing vegetation as green, clear water as dark blue, and muddy water as red. The tide was low, exposing mud flats and eel grass. The area of Boundary Bay is indicated by the *red box* (modified from *Rabinovich et al.* [2003]).

Unconsolidated sediments deposited off Roberts Bank produce an unstable delta front. Two very general types of failure may occur in this region: (1) Shallow, retrogressive flow-slide failures, and (2) deep-seated large-scale rotational failures [*Hamilton and Wigen*, 1987]. Several known flow slides occurred in the Fraser River delta between 1970 and 1985 [*McKenna and Luternauer*, 1987, *McKenna et al.*, 1992; *Chillarige et al.* 1997]. A failure in July 1985 was documented by *McKenna et al.* [1992] who assumed that the failure was a "*slow retrogressive flow over a period of hours*" so that no tsunamis were generated. However, according to *Hamilton and Wigen* [1987] and *Dunbar and Harper* [1993], more rapid (second-type failures) may generate substantial tsunamis with amplitudes exceeding several meters.

Rabinovich et al. [2003] numerically simulated a potential slide-generated tsunami in the southern Strait of Georgia. Guided by available qualitative information about the region, they postulated a failure of 0.75 km^3 for the edge of Roberts Bank occurring at a depth of about 100 m (the zone of postulated sensitive clays) and extending 7 km along the delta front between Canoe Passage and the BC Ferry Terminal, with a swath width of 3 km. The computed maximum tsunami wave heights along the northeastern and southwestern coasts of the strait for this failure are shown in Figure 11.

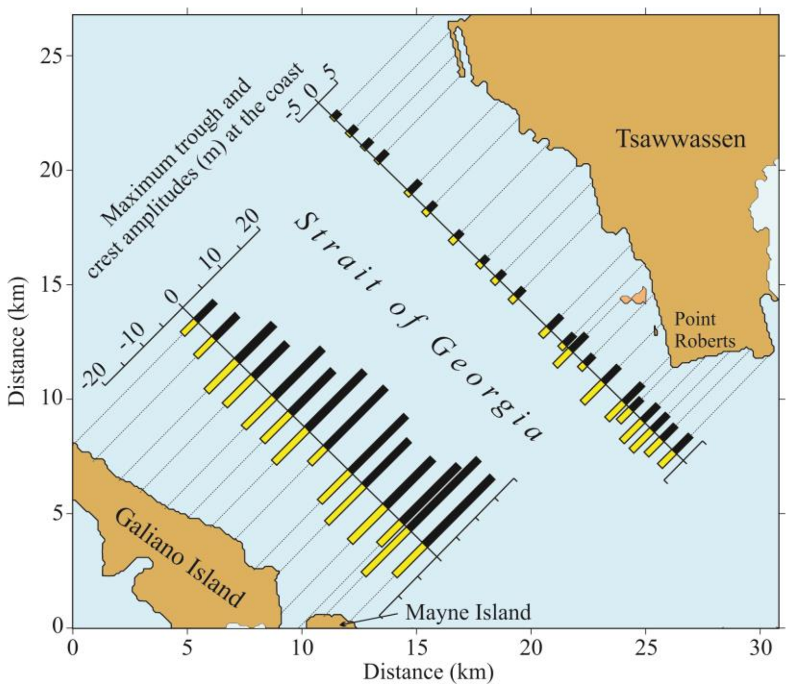

Figure 11. Maximum negative (trough) and positive (crest) wave amplitudes computed along the western and eastern coasts of the southern Strait of Georgia for Case 1 at high tide. (Modified from *Rabinovich et al.* [2003]).

An important aspect of the modelled tsunami wave field is that Roberts Bank efficiently reflects the waves and protects the mainland coast. Therefore, maximum waves are observed opposite the source area, rather than on the northeast coast of the strait near the initial failure zone. The computational domain used by *Rabinovich et al.* [2003] did not include the Boundary Bay region, however it appears that the region is protected from extreme shoreward propagating waves by a very shallow and wide shelf area bordering the eastern coast of the southern Strait of Georgia that effectively reflects these waves.

An additional zone of potential landslides and associated strong, even destructive, tsunamis, is Puget Sound. *González et al.* [2003] discussed this question in detail. The corresponding working group identified three distinct landslide situations that could result in a tsunami affecting local communities bordering Puget Sound: (1) submarine landslides on delta fronts; (2) submarine slides elsewhere in the Sound; and (3) slides from adjacent uplands. Submarine landslides can originate on the delta slopes of major rivers flowing into the Sound, in particular the Nisqually, Puyallup, Duwamish, and Snohomish rivers. Additional landslides can originate on steep submarine slopes of Puget Sound that are not part of a delta. Subaerial landslides that fall into Puget Sound with sufficient volume and velocity tidal conditions can generate large water waves with maximum heights that can reach several meters and even tens of meters. Such a tsunami was generated by a landslide at the Tacoma Narrows that occurred after the 1949 M_s 7.1 Olympia earthquake. However, the effects of Puget Sound tsunamis are **local** and the San Juan and Gulf islands partially protect areas, such as Boundary Bay, from possible effects of these tsunamis. On the contrary, the Boundary Bay region is not fully protected from landslide-generated tsunamis originating on the northern slopes of the San Juan Islands. Numerical simulations by *Nemati et al.* [2023] show that a possible “worst-case”, 0.17 km^3 rigid subaerial failure on the steep northeast coast of Orcas Island, close to the Holocene active Skipjack Island fault zone, would lead to runup of up to 7.5 m and strong currents of up to 4 m/s in Semiahmoo Bay and Birch Bay. Point Roberts, Boundary Bay and White Rock would experience lower wave effects, with maximum waves of around 1 m and runup of up to 3.5 m.

With the exception of an Orcas Island failure, a Roberts Bank slide-generated tsunamis presents markedly higher danger for the southern Strait of Georgia than those arriving from Puget Sound. However, this question needs additional research based both on detailed geophysical and geomorphological analyses of unstable alluvial sediment masses in this region and comprehensive numerical modelling, similar to the comprehensive modelling study by *Nemati et al.* [2023] for a possible failure on Orcas Island.

6. STORM SURGES AFFECTING THE BOUNDARY BAY REGION

A storm surge (a “meteorological ocean tide” [*Murty,* 1984]) is a coastal flood associated with low-pressure weather systems, such as cyclones, typhoons, and hurricanes. Surges mostly arise from the atmospheric pressure drop and strong onshore winds. Important factors promoting strong surges, are an extensive shallow shelf and coastal regions, like in the Bay of Bengal, the Gulf of Mexico or the Azov Sea, where hazardous storm surges occur regularly.

Storm surges are one of the deadliest natural disasters. The storm surge in the Bay of Bengal caused by the 1970 Bhola cyclone killed around 500,000 people on the coasts of the bay (two times more than the catastrophic 2004 Sumatra tsunami) and triggered a war between India and Pakistan. The May 2008 Nargis storm surge in the same region, the strongest in the 21st century, killed more than 138,000 people in Myanmar. The August 2005 Katrina hurricane in the Gulf of Mexico produced an enormously destructive surge that flooded a large part of the Louisiana coast, killed 1836 people and produced damage of $125 billion (in 2005 US dollars); the maximum surge height in southern Mississippi was >8.5 m.

The southern Strait of Georgia is vulnerable to storm surges. Using sea level measurements at the Point Atkinson tide gauge, *Forseth* [2012] investigated the highest recorded sea levels and selected 21 sea level flooding events that had occurred between 1960 and 2011. Three of these events resulted in significant flooding and damage. Two events, those of 16 December 1982 and 4 February 2006, caused approximate damage in excess of $2,000,000 (in 2011 Canadian Dollars).

The main focus of *Forseth* [2012] was the area of Metro Vancouver. However, he indicated that some of these events affected Boundary Bay and mentioned also some damage that occurred there. The most serious events were on 6 December 1967, 16 December 1982, and 4 February 2006. Extensive information on the latter event was collected by *Romanowski* [2010] who examined risk perceptions and coping strategies of Boundary Bay and Beach Grove residents during the storm. From 21 events analysed by *Forseth* [2012], one occurred in October, one in March and all the others in November–February; it appears that the highest risk of strong surges is related to these specific months.

Soontiens et al. [2016] examined and numerically simulated storm surges in the southern Strait of Georgia. They used a curvilinear orthogonal numerical grid with a grid spacing of approximately 440 m by 500 m and 40 vertical *z*-levels. The focus was on hindcasting of the destructive event of 4 February 2006 and a few other events. It was shown that surges entering the domain from the Pacific Ocean make the most significant contribution to surge amplitude within the Strait of Georgia. Atmospheric pressure forcing was found to be the dominant factor in surge amplitudes in this region, while local wind patterns caused a slight increase in surge amplitude on the mainland side of the Strait of Georgia. *Zhai et al.* [2019] demonstrated the effectiveness of reanalysis wind and sea level air pressure data to forecast storm surges in this region. The study also indicated the importance of steric effects and baroclinic dynamics for large-scale sea level variability. The *Zhai et al.* [2019] model domain included a major fraction of the northeast Pacific and extended from 30° to 61.4°N and from 122° to 180°W. The model resolution was 1/16°, corresponding to a resolution of about 7 km.

The studies of *Soontiens et al.* [2016] and *Zhai et al.* [2019] examined formation of storm surges in the Strait of Georgia, without focussing on the Boundary Bay region, a region examined in more detail by *Fine and Thomson* [2020c]. The authors used a two-dimensional (2-D) wetting-and-drying (WAD) version of the Princeton Ocean Model (POM) to examine storm-induced sea levels (storm surge) in Boundary Bay and in the adjacent areas of the Strait of Georgia. The model was based on a two-stage nested grid system, with high-resolution (3 m) bathymetric and topographic data in the Boundary Bay region: the outer grid (Grid 1) included Vancouver Island and the northwest US coast (Figure 12a), and spanned 47.2° – 51.4°N, 129.8° – 122.2°W, with a spatial resolution of about 370 m. The inner grid (Grid 2), which covered waters surrounding Metro Vancouver and Boundary Bay (Figure 12b), had a grid size of approximately 60 m. The model was driven at the outer coastal boundary by hourly atmospheric reanalysis time series; daily mean basin-scale steric sea level data at the outer boundary were applied to take into account large-scale open ocean effects. The model hindcasting capability was estimated by comparing numerically simulated sea level time series with actual tide gauge records during the storm surge of 20 December 2018. Figure 12 presents maps of the computed maximum sea level elevation during the event, while Figure 13, as an example, shows simulated and observed sea levels during this event for two stations, Victoria and Point Atkinson. Computations from three models are shown: (1) From the UBC model described by *Soontiens et al.* [2016]; (2) from the *Fine and Thomson* [2020c] model based on ERA5 - Europe’s global high-resolution atmospheric reanalysis; and (3) from the *Fine and Thomson* [2020c] model using HRDPS – Canada’s High Resolution Deterministic Prediction System. The latter model gives the best results for all stations.

According to the *Fine and Thomson* [2020c] model, the storm surge lasted for roughly one day and reached maximum heights (independent of the tide) of **0.6 m** in the northwest corner of Boundary Bay. Lower storm surge heights of around **0.5 m** were generated at Semiahmoo First Nations sites. The highest simulated storm surge of over **0.6 m** was obtained for the northern Strait of Georgia. These heights are to be added to the local tide height when estimating the total water depth during a storm surge. Based on these initial results, the model POM2D-WAD with HRDPS input forcing is able to accurately reproduce storm surge events in the Strait of Georgia and on the west coast of Vancouver Island.

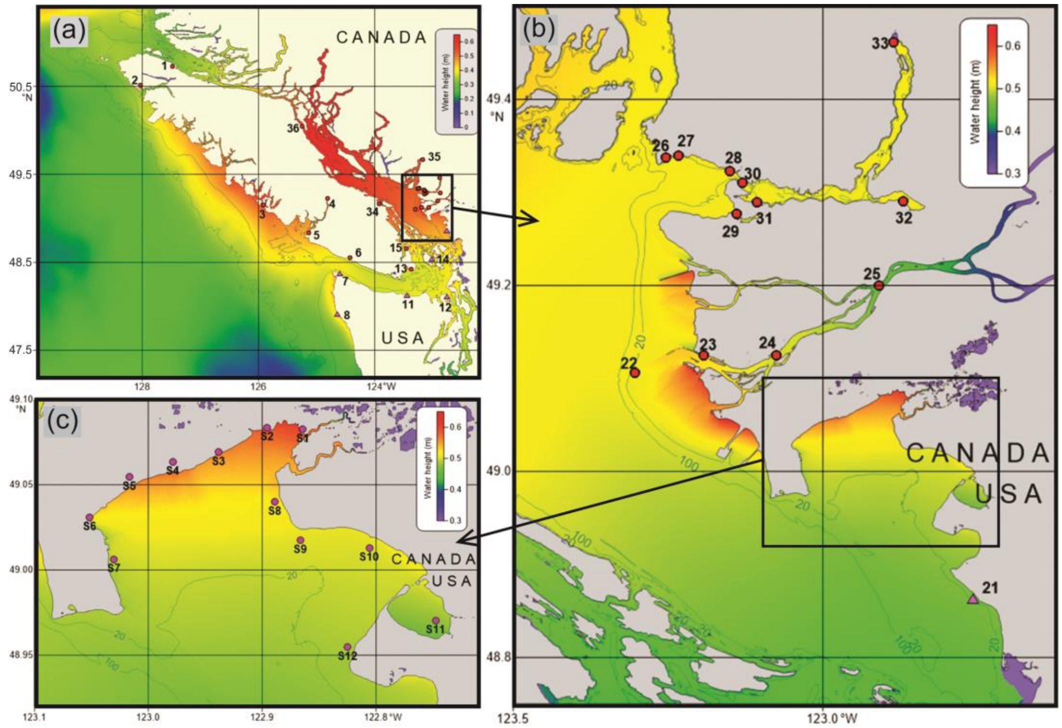

Figure 12. Maps of the maximum modeled sea level during the storm surge of 20 December 2018. (a) Grid 1 domain; shown are the locations of the CHS and NOAA tide gauges: 1 – Port Hardy, 2 - Winter Harbour, 3 – Tofino, 4 – Port Alberni, 5 – Bamfield, 6 – Port Renfrew, 7 – Neah Bay, 8 – La Push, 11 – Port Angeles, 12 – Port Townsend, 13 – Victoria, 14 – Friday Harbor, 15 – Patricia Bay, 34 – Nanaimo, 35 – Darrel Bay, and 36 – Campbell River; (b) Grid 2 domain, 22 – Sand Heads, 23 – Steveston, 24 - Woodwards Landing, 25 - New Westminster, 26 - Point Atkinson, 27 – Sandy Cove, 28 – Ambleside, 29 – Kitsilano, 30 - Calamity Point, 31 – Vancouver, 32 – Port Moody, and 33 - Indian Arm; (c) expanded map of the Boundary Bay region, also shown are the locations of Sites S1 to S12 for the modeled output (Modified from *Fine and Thomson* [2020c]).

Because storm surges caused by strong atmospheric depressions can differ owing to differences in individual cyclonic parameters (e.g., wind speed and direction, pressure distribution, spatial extent), it would be informative to model several other intense historical events to estimate the common and specific features of the storm surge distribution in Boundary Bay and estimate possible risk of storm surge to the area. The future effects of global sea level rise should be also taken into account.

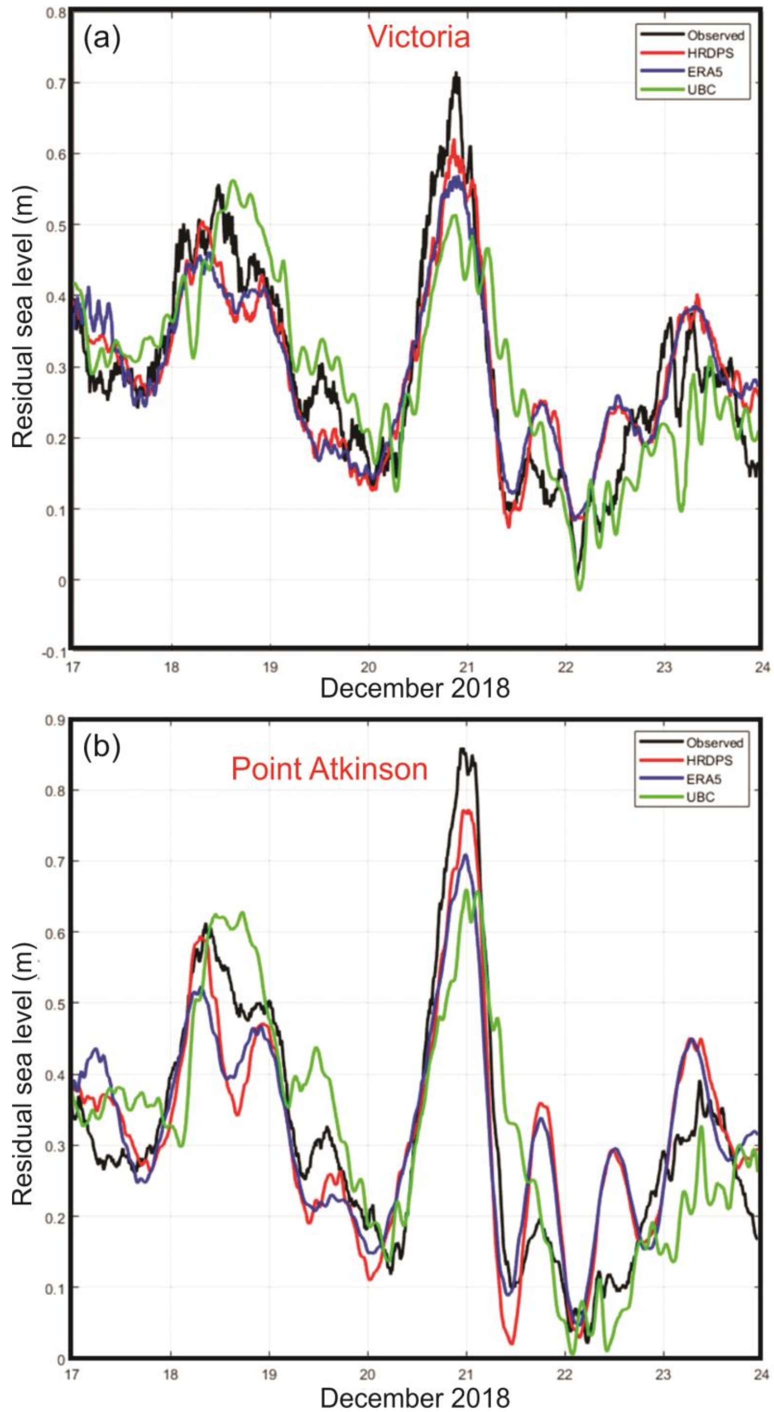

Figure 13. Comparison of the modeled sea level versus the observed records (black curve) at (a) Victoria and (b) Point Atkinson for HRDPS (red curve) forcing, ERA5 forcing (blue curve), and the UBC Salish Sea Storm Surge model (green curve). (Modified from *Fine and Thomson* [2020c]).

7. METEOROLOGICAL TSUNAMIS IN THE BOUNDARY BAY REGION

Recent observations from around the world and the occurrences of several devastating events, including the 2017-2018 meteotsunamis in the Netherlands, Durban (RSA) and Florida (USA), have demonstrated that meteotsunamis are much more common and widespread than was previously thought [*Pattiaratchi and Wijeratne*, 2015; *Rabinovich*, 2020]. The latest tragic event in the Persian Gulf of 19 March 2017, when 5 people were killed on the coast of Dayyer, Iran [cf. *Heidarzadeh et al.,* 2021], once again showed the serious threat of this phenomenon for coastal areas. Several major meteotsunami events were detected on the coast of southern British Columbia [*Thomson et al.,* 2009; *Stephenson and Rabinovich*, 2009; *Rabinovich et al.*, 2020a, 2021].

To estimate the potential meteotsunami risk for the Boundary Bay region, *Rabinovich et al.* [2019a] collected and examined all available high-resolution sea level records from three tide gauges located nearby (Figure 1): Point Atkinson (CHS), Cherry Point and Friday Harbor (NOAA). Their analysis showed that tsunami-like sea level events generated by high-frequency air pressure disturbances (meteotsunamis) regularly occur in the southern part of the Strait of Georgia, mostly in winter. The maximum recorded wave heights were minor: 16.7 cm (Cherry Point), 17.2 cm (Friday Harbor) and 13.1 cm (Point Atkinson). Although none of the events appear to have affected Boundary Bay, additional data inside the bay and high-resolution numerical modelling are required for reliable determination of the meteotsunami risk for the region. It should be emphasized that even relatively weak meteotsunamis can produce detectable, sometimes destructive, currents.

Unfortunately, no sea level or current velocity data are available for Boundary Bay. Therefore, to obtain estimates of expected meteotsunamis in this region, *Rabinovich et al.* [2020c] constructed a numerical model of this phenomenon for the southern Strait of Georgia, focussing on the Boundary Bay region. The model was verified using data from the meteotsunami of 1 November 2010 [*Rabinovich et al.*, 2020a, 2021]. School network data [*Weaver and Wiebe*, 2006] were used to derive the physical parameters (propagation speed and direction) of atmospheric disturbances propagating over the region; these parameters were applied to force numerical simulations of the event and the results were compared to observations from selected tide gauge sites. The numerical experiments revealed strongly individual sea level responses at each site to changing air pressure disturbance speed, direction and intensity, such that each location has its own set of “site-specific” air pressure characteristics that produce the strongest sea level response. Differences in the local topography and coastline geometry appear to be responsible for the different responses among sites.

The numerical model was then used to simulate meteotsunamis in the Boundary Bay region. A wide range of disturbance propagation speeds was considered, from 10 to 70 m/s, with an increment of 5 m/s, along with a full circle of propagation directions, with azimuths from 0º to 360º True at an increment of 10º. As an example, Figures 14 and 15 show maximum computed sea level heights and current velocities for the disturbance propagation speed, U = 35 m/s, and four selected disturbance directions (from 210º, 240º, 270º and 300º True) that correspond to common atmospheric disturbances in the Boundary Bay region, which are westerly and southwesterly (i.e., propagating in the NE and E directions).

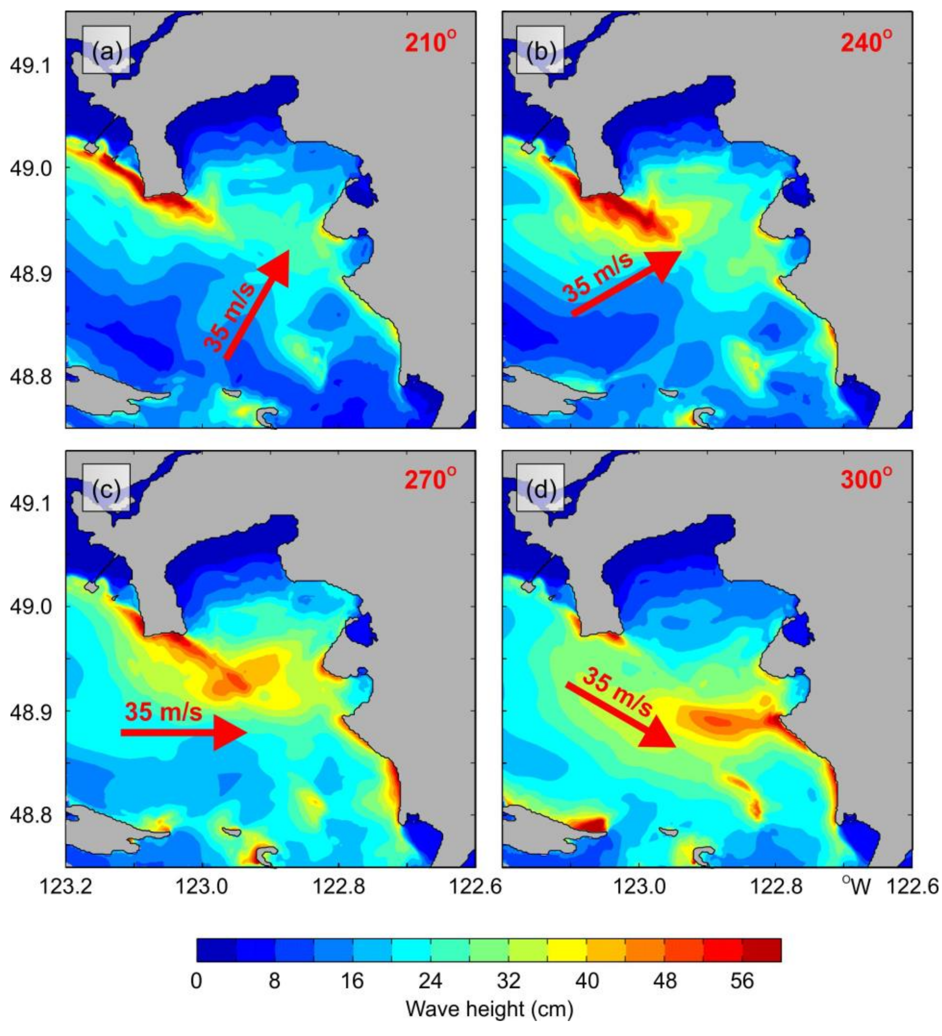

Figure 14. Maximum sea level wave heights for the Boundary Bay region computed for the propagation disturbance speed of 35 m/s and four disturbance directions: from 210º, 240º, 270º and 300º True.

The maximum height of generated oscillations increases offshore: from 5-6.5 cm to 31 at the shelf-break and 51 cm at the entrance to the bay. The shelf-break was found to effectively shelter the inner part of the bay. The coastal geometry and local bathymetry of Boundary Bay appear to strongly attenuate the incoming waves, making this region well sheltered from significant meteotsunamis. Meteotsunami-generated currents for the region of Boundary Bay are weak (maximum currents are up to 11.5 cm/s) and not dangerous.

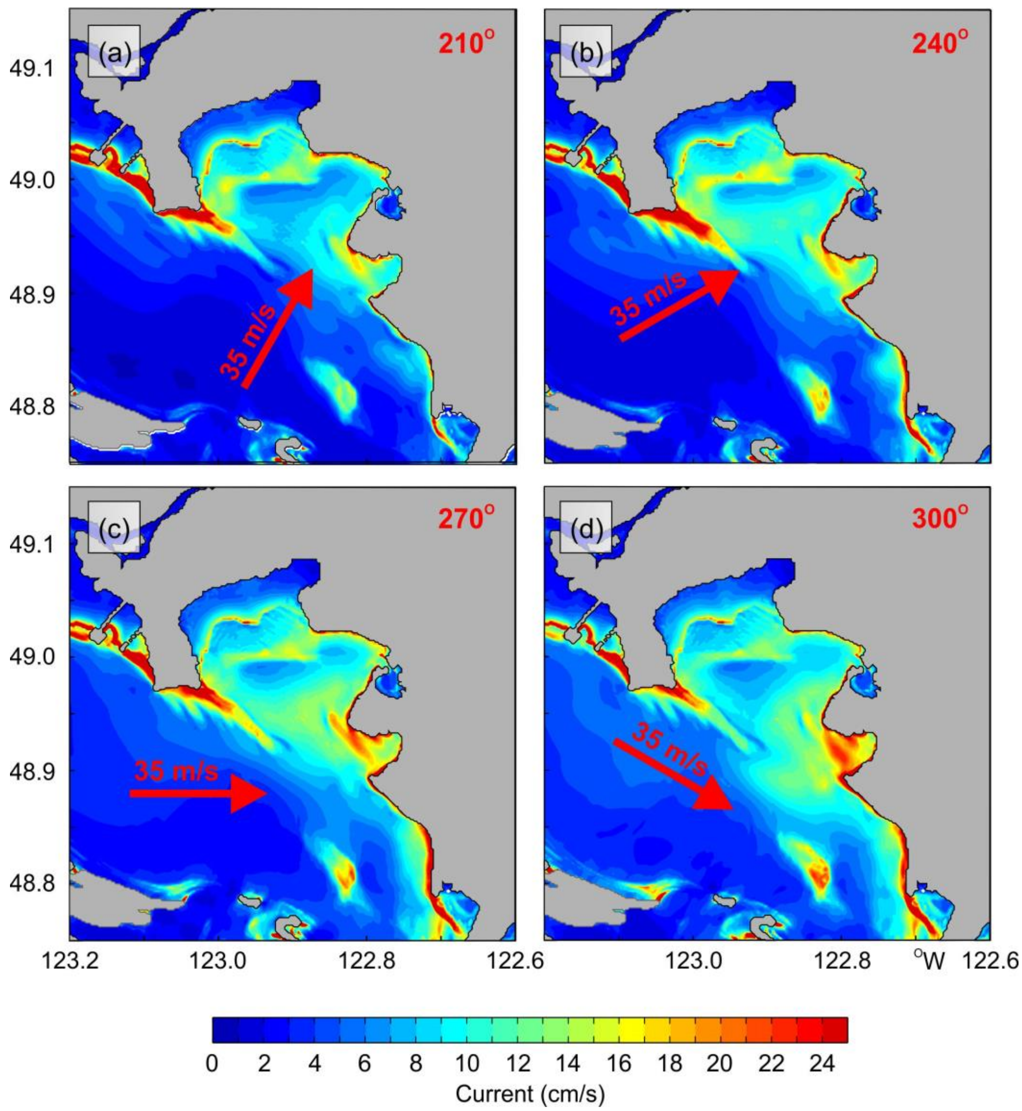

Figure 15. The same as in Figure 14 but for the maximum current speeds.

The results of the computations demonstrate that the propagation direction is not critical: the general character of simulated wave fields and maximum sea heights and current velocities are alike for all four selected disturbance directions; the most effective direction is from 300º True. The differences between computed wave fields for different disturbance speeds are much more significant. The maximum wave heights for U = 35 m/s of more than 50-55 cm occur on the coast of Point Roberts, the southernmost tip of the Tsawwassen Peninsula (Figure 14), and along the shelf-break at the entrance to Boundary Bay. It is clear that the shelf-break effectively reflects the incoming waves, hindering meteotsunamis from penetrating into the bay and reaching the northwest coast.

In summary, the spatial fields of maximum computed sea level heights and current speeds demonstrate that the local topography of Boundary Bay shelters the region from incoming waves, protecting the bay from sea level oscillations and currents associated with meteotsunamis generated in the southern Strait of Georgia.

8. CONCLUSIONS

The present report summarizes previous major results and findings related to various types of hazardous sea level variations in the Strait of Georgia, with particular emphasis on the Boundary Bay region. We conclude that there are five types of marine sea level hazards that potentially can affect the area of Boundary Bay:

(1) Major trans-oceanic tsunamis

(2) Local tsunamis

(3) Landslide-generated tsunamis

(4) Storm surges

(5) Meteorological tsunamis

The "Summary" is based on our previous reports related to this region, NOAA reports on Puget Sound, Juan de Fuca Strait and the southern part of the Strait and on published papers investigating sea level variations in this region through analyses of available observational data and numerical simulations.

An important factor influencing the character of sea level oscillations in Boundary Bay is the local topography. The San Juan and Gulf islands effectively shelter the bay from perilous waves coming from the open ocean, Puget Sound and partly from the northern Strait of Georgia. An additional factor protecting Boundary Bay is the shelf-break, which reflects waves arriving at the bay. From this aspect, the Boundary Bay region is relatively safe compared to other British Columbia coastal regions.

A summary of all types of sea level hazard affecting the coast of Boundary Bay is given in Table 1. This summary enables us to estimate the relative importance of the various types of sea level events and the strength of their associated currents.

Table 1. Maximum expected sea level wave amplitudes and current speeds in Boundary Bay associated with various types of hazardous sea level events

Sea level type	Peak sea level amplitude (m)		Max current speed (m/s)	Comments
	NW Boundary Bay	Semi-ahmoo		
Major trans-oceanic tsunamis				
CSZ	1.5	1.3	3.0[1] and 2.0[2]	[1]Drayton Harbour entrance;
Alaska	0.45	0.35	1.5[1] and 0.5[2]	[2]Campbell River mouth
Local tsunamis	< 0.25	< 0.25	< 0.5	-
Landslide tsunamis	?	?	?	Needs additional analysis and numerical modelling
Storm surges	0.6	0.5	< 0.5	-
Meteotsunamis	0.25	0.25	0.5	-

Of the five types of sea level variations listed above, the most hazardous for the Boundary Bay region are major trans-oceanic tsunamis, more specifically, tsunamis generated in two regions adjacent to British Columbia: (1) the Cascadia Subduction Zone (CSZ) and (2) the Alaska-Aleutian Subduction Zone. A high-resolution, four-level, nested-grid tsunami model with spatial resolution of ~1.85 km (Grid 1), 360 m (Grid 2), 60 m (Grid 3), and 10 m (Grid 4) was used by *Fine and Thomson* [2020a, 2020b] to simulate tsunami waves and wave-induced currents generated in Boundary Bay by these two possible major events.

For a future CSZ failure, the tsunami impacting Boundary Bay is expected to reach maximum wave amplitudes of **up to 1.5 m** in the northwestern part on the bay and **up to 1.3 m** along the

Semiahmoo coast. The tsunami-induced ocean currents will typically be **less than 1 m/s** in most areas but **up to 3 m/s** at the entrance to Drayton Harbor and **up to 2 m/s** at the mouth of Campbell River on the Semiahmoo coast. Tsunami waves would cause flooding, mostly in the northwestern part of Boundary Bay; in the Semiahmoo area the flooding would likely occur in the Campbell River valley but will have a limited effect. Adding a 50% safety factor (a typical engineering value [cf. *AECOM*, 2013]), the tsunami hazard to the Semiahmoo area remains confined to the low-lying regions along the Campbell River.

Tsunami waves arising from a major Alaska earthquake are expected to be weaker in Boundary Bay than those associated with a CSZ tsunami. The modelling results of *Fine and Thomson* [2020b] show that the tsunami in this region will reach **0.45 m** above the tidal level, with the first wave being the highest. Wave heights along the Semiahmoo coast will be up to **0.35 m**. The tsunami will induce moderate currents at the entrance of Drayton Harbor (up to **1.5 m/s**) and at the mouth of Campbell River (up to **0.5 m/s**). *Fine and Thomson* [2020b] recommend applying a safety factor of 50% for a 1964-type event. However, even with such a factor, the risk of flooding in Boundary Bay by Alaska 1964-type tsunami is low compared with that from a CSZ 1700-type tsunami.

Tsunami waves triggered by local sources in the Strait of Georgia and Puget Sound were found to be of a minor risk for Boundary Bay. The strongest known earthquake in this region, the 1946 Vancouver Island earthquake with epicenter near Campbell River (M_w 7.3), produced a tsunami that had only a local effect. The Boundary Bay region is well sheltered from tsunamis originating in Puget Sound and the northern Strait of Georgia by the Gulf and San Juan islands.

The contribution of storm surge to marine hazards in Boundary Bay was examined numerically by *Fine and Thomson* [2020c]. According to their high-resolution model, which takes into account wetting and drying effects, storm surge in this region can reach maximum heights (independent of the tide) of **0.6 m** on the northwest coast of Boundary Bay and around **0.5 m** at Semiahmoo First Nations sites. These heights are to be added to the local tide height when estimating the total water depth during a storm surge.

Another type of sea level oscillation occurring in Boundary Bay are meteorological tsunamis (tsunami-like waves generated by atmospheric processes). However, the results of both data analysis [*Rabinovich et al.,* 2019a] and numerical modelling [*Rabinovich et al.,* 2020c] show that they have minor effects in this region (wave amplitudes **<25 cm**), mostly because of the reflecting effect of the shelf-break at the entrance to the bay. The associated currents are maximum (>0.5 m/s ~ 1 knots) at the shelf-break but are weak near the coast.

Landslide-generated tsunamis in the southern Strait of Georgia and their possible effect on Boundary Bay require additional investigation and numerical modelling. In the vicinity of Roberts Bank, at the entrance to the Fraser River Delta, a large body of unconsolidated alluvial sediments has accumulated [cf. *Chillarige et al.*, 1997; *Christian et al.*, 1997]. Underwater slides have occurred in this region in the past and are likely to occur in the future [*Hamilton and Wigen*, 1987; *Bornhold and Thomson*, 2012]. Whether the slides will have the character of shallow, retrogressive flow-slide failures or deep-seated large-scale rotational failures is questionable. Substantial geophysical, geomorphological and marine geological studies are needed to clarify this problem. Detailed, high-resolution numerical modelling of tsunami waves from possible source regions are required, such as that conducted by *Nemati et al.* [2023] for an earthquake-initiated failure on the northeastern slope of Orcas Island in the San Juan Islands.

REFERENCES

AECOM (2013), *Modelling of Potential Tsunami Inundation Limits and Run-Up,* Capital Regional District, Project No. 6024 2933, 36 p.

Atwater, B.F., Musumi-Rokkaku, S., Satake, K., Tsuji, Y., Ueda, K., and Yamaguchi, D.K., (2005), *The Orphan Tsunami of 1700—Japanese Clues to a Parent Earthquake in North America*, U.S. Geological Survey Professional Paper No. 1707, 133 p.

Bornhold, B.D. and Thomson, R.E. (2012), Tsunami hazard assessment related to slope failures in coastal waters. In *Landslides - Types Mechanisms and Modelling*, Eds. John Clague and Douglas Stead, Cambridge University Press, pp. 108-120.

Chillarige, A.V., Morgenstern N.R., Robertson, P.K., and Christian H.A. (1997), Seabed Instability due to Flow Liquefaction in the Fraser River Delta, *Canadian Geotechnical Journal 34,* 520-533.

Christian, H.A., Mosher, D.C., Mulder, T., J.V. Barrie, and Courtney R.C. (1997), Geomorphology and potential slope instability on Fraser River delta foreslope, Vancouver, British Columbia, *Canadian Geotechnical Journal 34*, 432-446.

Clague, J.J., Bobrowsky, P.T., and Hutchinson, I., (2000), A review of geological records of large tsunamis at Vancouver Island, British Columbia, and implications for hazard, *Quaternary Science Reviews 19*, 849-863.

Clague, J.J., Munro, A., and Murty, T.S. (2003), Tsunami hazard and risk in Canada, *Natural Hazards, 28* (2-3), 407-434.

Dengler, L., Uslu, B., Barberopoulou, A., Borrero, J., and Synolakis, C. (2008), The vulnerability of Crescent City, California, to tsunamis generated by earthquakes in the Kuril Islands region of the northwestern Pacific, *Seismological Research Letters 79*(5), 608-619.

Dunbar, D., LeBlond, P., and Murty, T.S. (1991), Evaluation of tsunami amplitudes for the Pacific coast of Canada, *Progress in Oceanography 26*, 115–177.

Dunbar, D.S. and Harper, J.R. (1993), Numerical simulation of tsunamigenic submarine slope failure in the Fraser River delta, British Columbia, *Marine Geodesy 16*, 101-108.

Fine, I.V. and Thomson, R.E. (2020a), *Numerical Simulation of a Cascadia Subduction Zone: Tsunami with Application to Boundary Bay in the Southern Strait of Georgia*, Canadian Technical Report of Hydrography and Ocean Sciences, Fisheries and Oceans Canada, Institute of Ocean Sciences, Sidney.

Fine, I.V, and Thomson, R.E. (2020b), *Numerical Simulation of an Alaska 1964-type Tsunami with Application to Boundary Bay in the Southern Strait of Georgia*, Canadian Technical Report of Hydrography and Ocean Sciences, Fisheries and Oceans Canada, Institute of Ocean Sciences, Sidney.

Fine, I.V., and Thomson, R.E. (2020c), *Numerical Simulation of Storm Surge in Boundary Bay in the Southern Strait of Georgia*, Canadian Technical Report of Hydrography and Ocean Sciences, Fisheries and Oceans Canada, Institute of Ocean Sciences, Sidney.

Forseth, P. (2012), *Adaptation to Sea Level Rise in Metro Vancouver: A Review of Literature for Historical Sea Level Flooding and Projected Sea Level Rise in Metro Vancouver*, Technical Report, ACT Adaptation to Climate Change Team, SFU.

Gao, D. (2016), *Defining Megathrust Tsunami Sources at Northernmost Cascadia Using Thermal and Structural Information*. Master of Science Thesis, School of Earth and Ocean Sciences, The University of Victoria; https://dspace.library.uvic.ca/handle/1828/7435

González, F.I., Sherrod, B.L., Atwater, B.F. et al. (2003), *Puget Sound Tsunami Sources—2002 Workshop Report*, NOAA OAR Special Report, Contribution No. 2526 from NOAA/Pacific Marine Environmental Laboratory.

Hamilton, T.S. and Wigen, S.O. (1987), The Foreslope Hills of the Fraser River delta: Implication of tsunamis in Georgia Strait, *Science of Tsunami Hazards* 5, 15-33.

Heidarzadeh, M. and Rabinovich, A.B. (2021), Combined hazard of typhoon-generated meteorological tsunamis and storm surges along the coast of Japan, *Natural Hazards*106 (2), 1639-1672; doi:10.1007/s11069-020-04448-0.

Johns, M.W., Prior, D.B., Bornhold, B D., Coleman, J.M., and Bryant, W.R. (1986), Geotechnical Aspects of a Submarine Slope Failure, Kitimat Fjord, British Columbia, *Marine Geotechnology* 6, 243–279.

Johnson, J.M., Satake, K., Holdahl, S.R., and Sauber, J. (1996), The 1964 Prince William Sound earthquake – joint inversion of tsunami waveforms and geodetic data, *Journal of Geophysical Research 101* (B1), 523-532.

Kulikov, E.A., Rabinovich, A.B., Thomson, R.E., and Bornhold, B.D. (1996), The Landslide Tsunami of November 3, 1994, Skagway Harbor, Alaska, *Journal of Geophysical Research, 101* (C3), 6609-6615.

Lander, J.F. (1996), *Tsunamis Affecting Alaska*, 1737-1996. USDC/NOAA, Boulder, CO, USA, 195 p.

Leonard, L.J., Rogers, G.C., and Mazotti, S. (2014), Tsunami hazard assessment of Canada, *Natural Hazards 70*, 237-274.

McKenna, G.T., and Luternauer, J.L. (1987), First documented large failure at the Fraser River delta front, British Columbia, *Geological Survey of Canada*, Pap.*87-1A*, 919-924.

McKenna, G.T., Luternauer, J.L., and. Kostaschuk, R.A. (1992), Large-scale mass-wasting events on the Fraser River Delta near Sand Heads, British Columbia, *Canadian Geotechnical Journal 29*, 151-156.

Murty, T.S. (1984), *Storm Surges – Meteorological Ocean Tides*, No. 212 Canadian Bulletin of Fisheries and Aquatic Sciences, Ottawa, 897 pp.

Murty, T.S. and Crean, P.B. (1986), Numerical simulation of the tsunami of June 23,1946 in British Columbia, Canada, *Science of Tsunami Hazards 4*(1), 15-24.

Murty T. S. and Hebenstreit G. T. (1989) Tsunami amplitudes from local earthquakes in the Pacific Northwest region of North America. Part 2: Strait of Georgia, Juan de Fuca Strait, and Puget Sound, *Marine Geodesy 13* (3), 189-209, doi: 10.1080/15210608909379623

Myers, E.P. and Baptista, A.M. (2001), Analysis of factors influencing simulations of the 1993 Hokkaido Nansei-Oki and 1964 Alaska tsunamis. *Natural Hazards 23*, 1-28; https://doi.org/10.1023/A:1008150210289

Nemati, F., Leonard, L., Thomson, R., Lintern, G., and Kouhi, S. (2023), Numerical modeling of a potential landslide-generated tsunami in the southern Strait of Georgia, *Natural Hazards* https://doi.org/10.1007/s11069-023-05854-w.

Pattiaratchi, C.B., and Wijeratne, S. (2019), Observations of meteotsunamis in Australia, The First World Conference on Meteotsunamis, Split, Croatia, 8-11 May 2019, Book of Abstracts, p. 26.

Rabinovich, A.B. (2020), Twenty-seven years of progress in the science of meteorological tsunamis following the 1992 Daytona Beach event, *Pure and Applied Geophysics 177*(3), 1193-1230; doi: 10.1007/s00024-019-02349-3.

Rabinovich, A.B., Thomson, R.E., Bornhold, B.D., Fine, I.V., and Kulikov, E.A., (2003), Numerical modelling of tsunamis generated by hypothetical landslides in the Strait of Georgia, British Columbia, *Pure and Applied Geophysics 160* (7), 1273-1313.

Rabinovich, A.B., and Stephenson, F.E. (2004), Longwave measurements for the coast of British Columbia and improvements to the tsunami warning capability, *Natural Hazards, 32* (3), 313-343.

Rabinovich, A.B., Thomson, R.E., and Stephenson, F.E., (2006), The Sumatra tsunami of 26 December 2004 as observed in the North Pacific and North Atlantic oceans, *Surveys in Geophysics 27*, 647-677.

Rabinovich, A.B., Thomson, R.E., and Šepić, J. (2019a), *Meteorological tsunamis on the south coast of British Columbia with application to Boundary Bay*, Canadian Technical Report of Hydrography and Ocean Sciences, Fisheries and Oceans Canada, Institute of Ocean Sciences, Sidney.

Rabinovich, A.B., Thomson, R.E., Krassovski, M.V., Stephenson, F.E., and Sinnott, D.C. (2019b), Five great tsunamis of the 20th century as recorded on the coast of British Columbia, *Pure and Applied Geophysics 176* (7), 2887-2924; doi: 10.1007/s00024-019-02133-3.

Rabinovich, A.B., Thomson, R.E., and Šepić, J. (2020a), *The meteorological tsunami of 1 November 2010 in the southern Strait of Georgia: A case study*, Canadian Technical Report of Hydrography and Ocean Sciences, Fisheries and Oceans Canada, Institute of Ocean Sciences, Sidney.

Rabinovich, A.B., Thomson, R.E., and Šepić, J. (2020b), *Historical tsunamis and other extreme longwave oscillations in the Strait of Georgia with focus on the Institute of Ocean Sciences (Patricia Bay) and Pacific Biological Station (Nanaimo) regions*, Canadian Technical Report of Hydrography and Ocean Sciences, Fisheries and Oceans Canada, Institute of Ocean Sciences, Sidney.

Rabinovich, A.B., Šepić, J., and Thomson, R.E. (2020c), *Numerical modelling of meteorological tsunamis in the southern part of the Strait of Georgia with application to Boundary Bay*, Canadian Technical Report of Hydrography and Ocean Sciences, Fisheries and Oceans Canada, Institute of Ocean Sciences, Sidney.

Rabinovich, A.B., Šepić, J., and Thomson, R.E. (2021), The meteorological tsunami of 1 November 2010 in the southern Strait of Georgia: A case study, *Natural Hazards106* (2), 1503-1544; doi: 10.1007/s11069-020-04203-5.

Rogers, G.C. (1980), A documentation of soil failure during the British Columbia earthquake of 23 June, 1946, *Canadian Geotechnical Journal 17*, 122–127.

Rogers, G.C. (1998), Earthquakes and earthquake hazard in the Vancouver area. In: J.J. Clague, J.L. Luternauer, and D.C. Mosher (Eds) *Geology and Natural Hazards of the Fraser River Delta, British Columbia*. Geological Survey of Canada, Bull. 525, 17–25.

Rogers, G C. and Hasegawa, H.S. (1978), A second look at the British Columbia earthquake of 23 June, 1946, *Bulletin of the Seismological Society of America 68* (3), 653–675.

Romanowski, S.A. (2010), *Storm Surge Flooding: Risk Perception and Coping Strategies of Residents*, Master's thesis, Edmonton.

Seemann, M., Onur, T., and Cloutier-Fisher, D. (2011), Earthquake shaking probabilities for communities on Vancouver Island, British Columbia, Canada, *Natural Hazards 58*, 1253-1273; doi 10.1007/s11069-011-9727-6.

Soontiens, N., Allen, S.E., Latornell, D. et al. (2016), Storm surges in the Strait of Georgia simulated with a regional model, *Atmosphere-Ocean 54* (1), 1-21,

Stephenson, F.E., Rabinovich, A.B., Solovieva, O.N., Kulikov, E.A., and Yakovenko, O.I., (2007), *Catalogue of Tsunamis, British Columbia, Canada: 1700-2007*. Preprint. P.P. Shirshov Inst. Oceanology, Moscow, 134 p.

Stephenson F.E., and Rabinovich, A.B. (2009), Tsunamis on the Pacific coast of Canada recorded in 1994-2007, *Pure and Applied Geophysics 166* (1/2), 177-210.

Suleimani, E.N., Nicolsky, D.J., and Koehler, R.D., (2013), *Tsunami Inundation Maps of Sitka, Alaska*, Report of Investigations 2013-3, State of Alaska, Department of Natural Resources, Division of Geological and Geophysical Surveys, Fairbanks, AK, 76 p.

Thomson, R. E., (1981), *Oceanography of the British Columbia Coast*. Can. Special Pub. Fish. Aquat. Sci., 56. Ottawa, 291 p.

Thomson, R.E., Rabinovich, A.B., Kulikov, E.A., Fine, I.V., and Bornhold, B.D. (2001), On numerical simulation of the landslide-generated tsunami of November 3, 1994 in Skagway Harbor, Alaska. In *Tsunami Research at the End of a Critical Decade*, edited by G. Hebenstreit, Kluwer Acad. Publ., Dordrecht, 243-282.

Thomson, R.E., Rabinovich, A.B., Fine I.V. et al. (2009), Meteorological tsunamis on the coasts of the British Columbia and Washington. *Physics and Chemistry of the Earth 34*, 971-988.

Walsh, T.J., Titov, V.V., Venturato, A.J., Mofjeld, H.O., and González, F.I. (2003), *Tsunami Hazard Map of the Elliott Bay Area, Seattle, Washington: Modeled Tsunami Inundation from a Seattle*

Fault Earthquake, Washington Division of Geology and Earth Resources, Open File Report 2003-14, NOAA TIME Center, PMEL, Seattle, WA.

Walsh, T.J., Arcas, D., Titov, V.V., and Chamberlin, C.C. (2014), *Tsunami Hazard Map of Everett, Washington: Model Results for Magnitude 7.3 and 6.7 Seattle Fault Earthquakes, Washington* Division of Geology and Earth Resources, Open File Report 2014-03, NOAA Center for Tsunami Research, PMEL, Seattle, WA.

Wang, K., Wells, R., Mazzotti, S., Hyndman, R.D., and Sagiya T. (2003), A revised dislocation model of interseismic deformation of the Cascadia subduction zone, *Journal of Geophysical Research 108*(B1), doi:10.1029/2001JB001227.

Wang, P-L., Engelhart, S.E., Wang, K., Hawkes, A.D., Horton, B.P., Nelson, A.R., and Witter, R.C., (2013), Heterogeneous rupture in the Great Cascadia earthquake of 1700 inferred from coastal subsidence estimates. *Journal of Geophysical Research 118*, 2460-2473.

Weaver AJ, Wiebe EC (2006) Micrometeorological network in Greater Victoria schools: www.victoriaweather.ca. *CMOS Bulletin 34*(4):184-190.

Zhai, L., Greenan, B., Thomson, R., and Tinis, S. (2019) Use of oceanic reanalysis to improve estimates of extreme storm surge, *Atmospheric and Oceanic Technology 36*, 2205-2219; doi:10.1175/JTECH-D-19-0015.1.